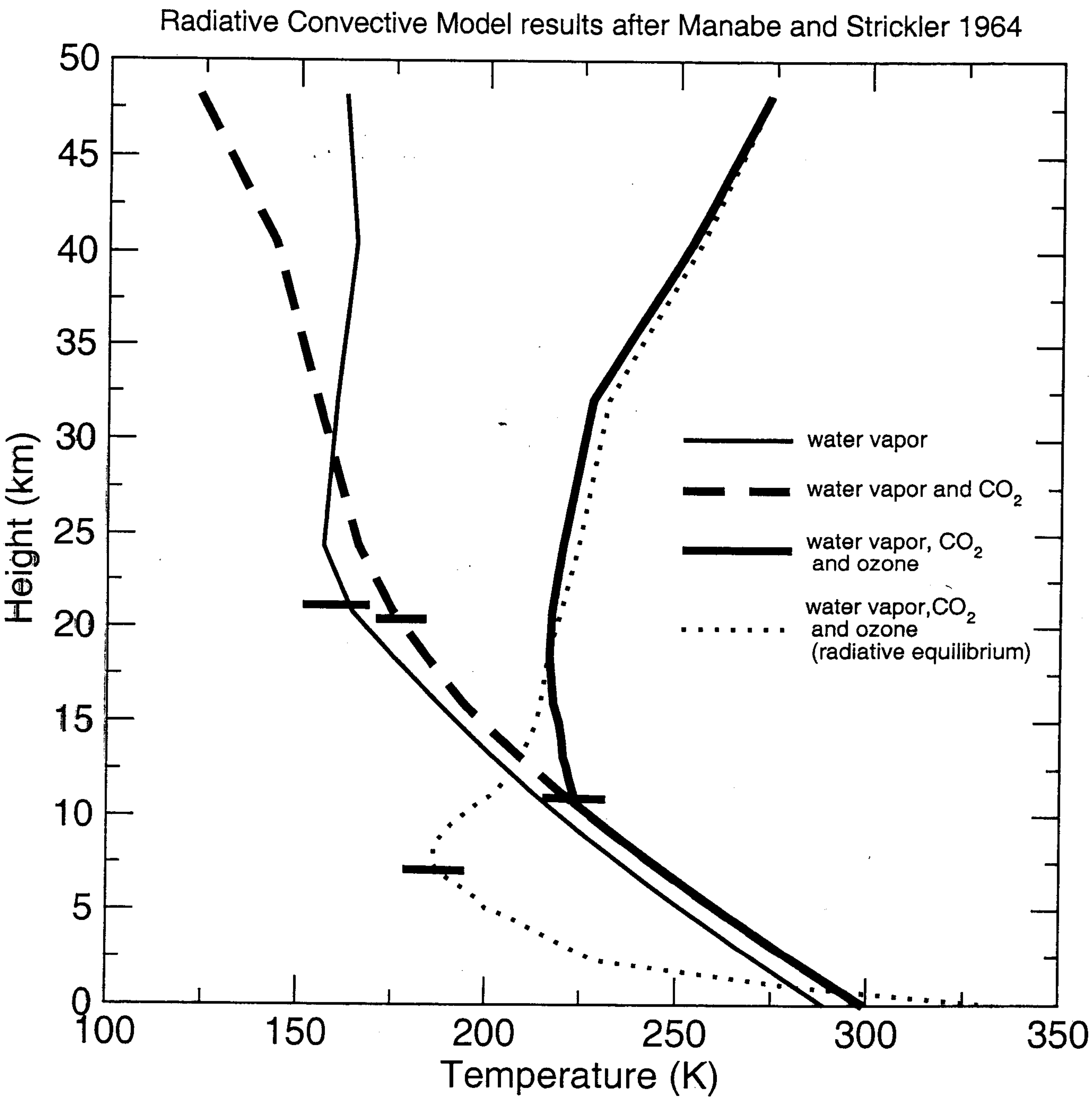

Courtesy of Piers Forster
(Reading Univ.)

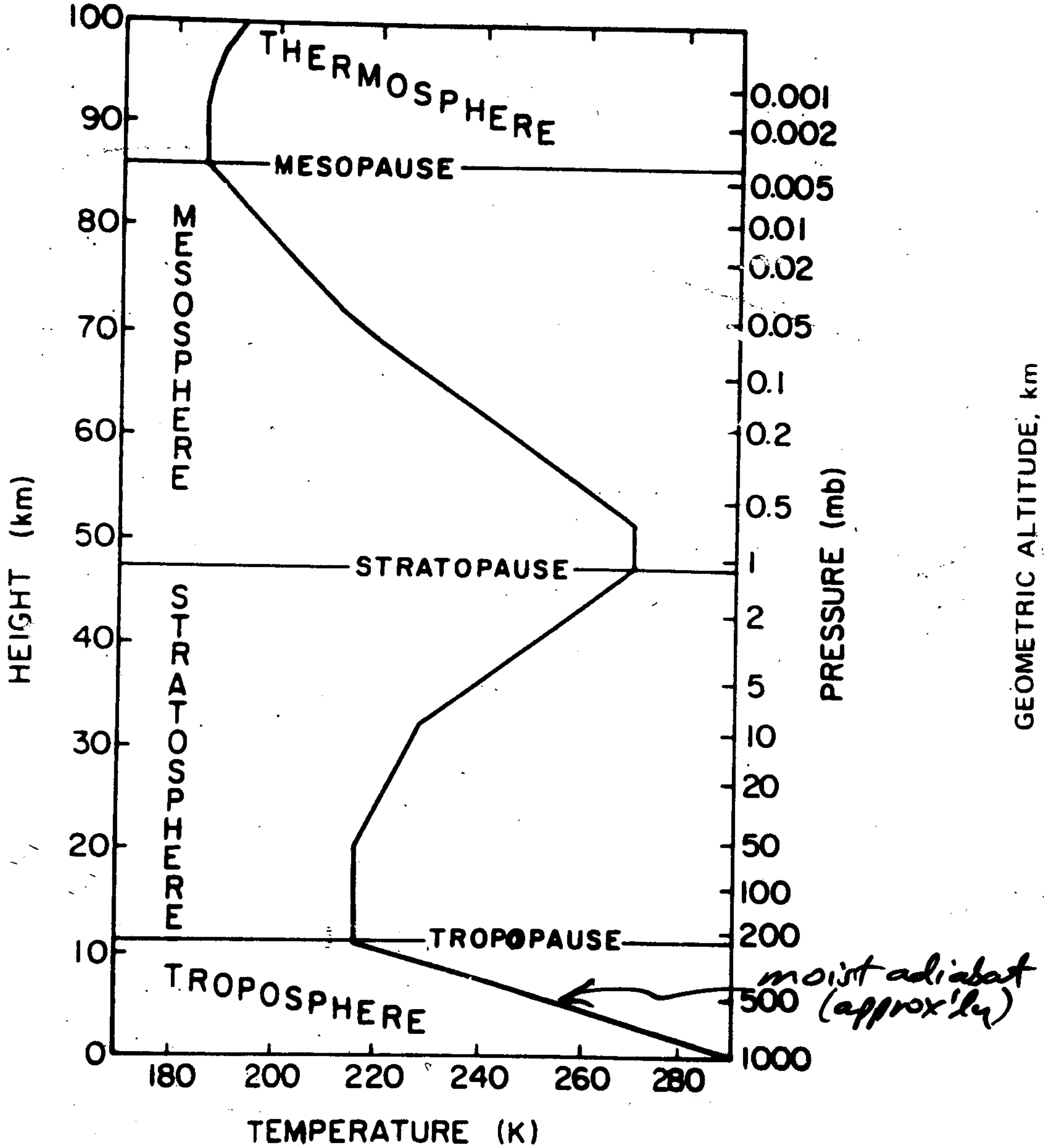

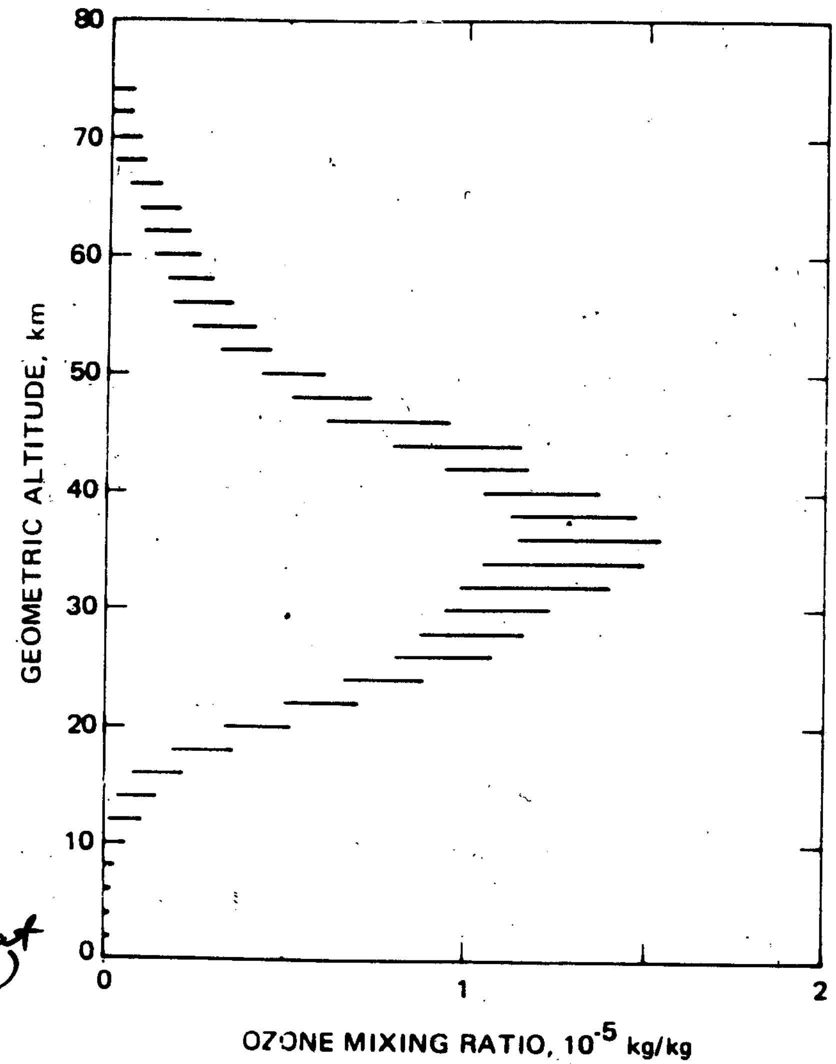

from Andrews, Holton & Leovy (1987)

Solid lines : potential temperature
Dashed lines : temperature

Troposphere : weak stratification
Stratosphere : strong stratification

from Holton et al. (1995)

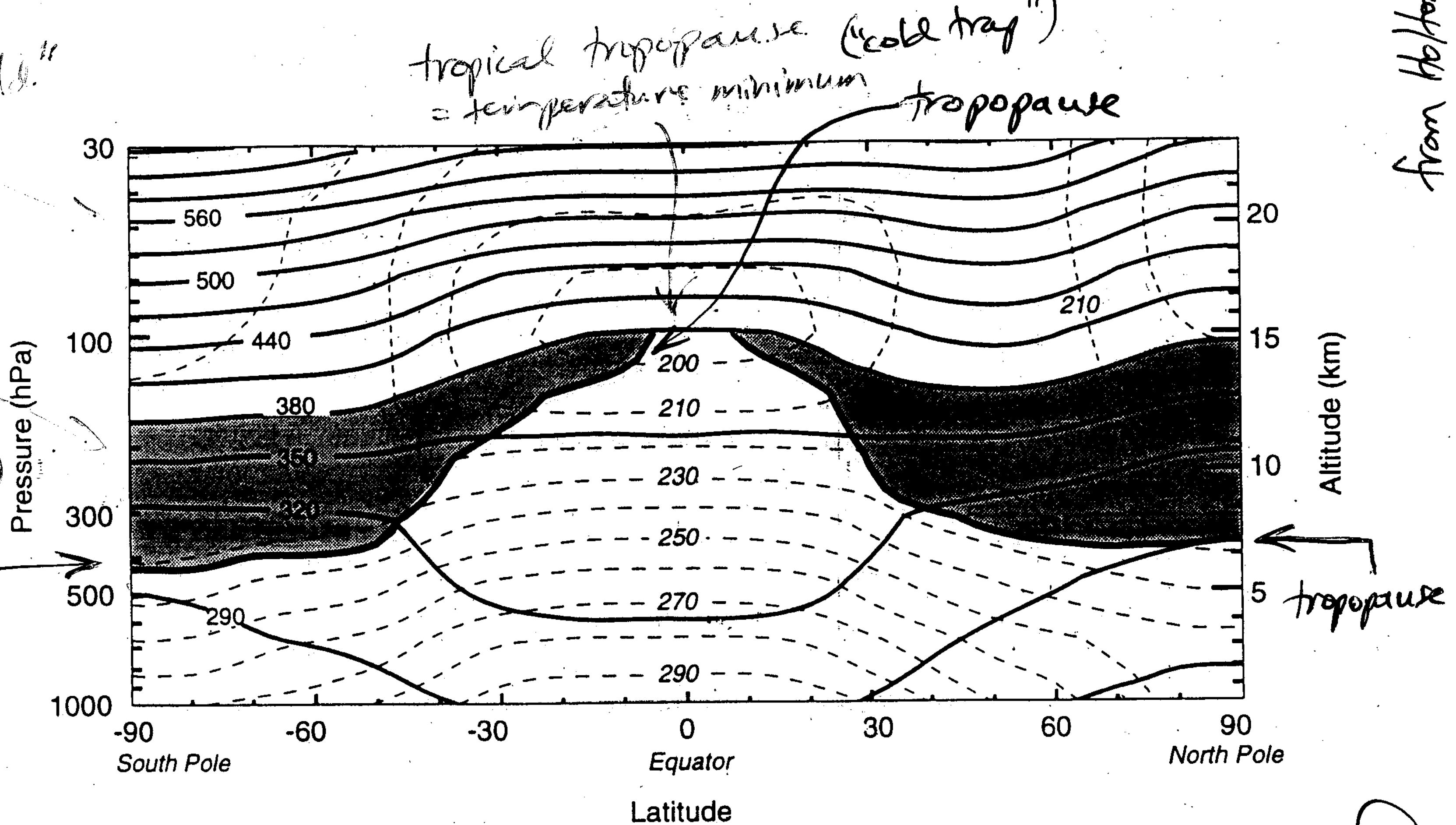

1

Radiative equilibrium of the middle atmosphere in January (X)

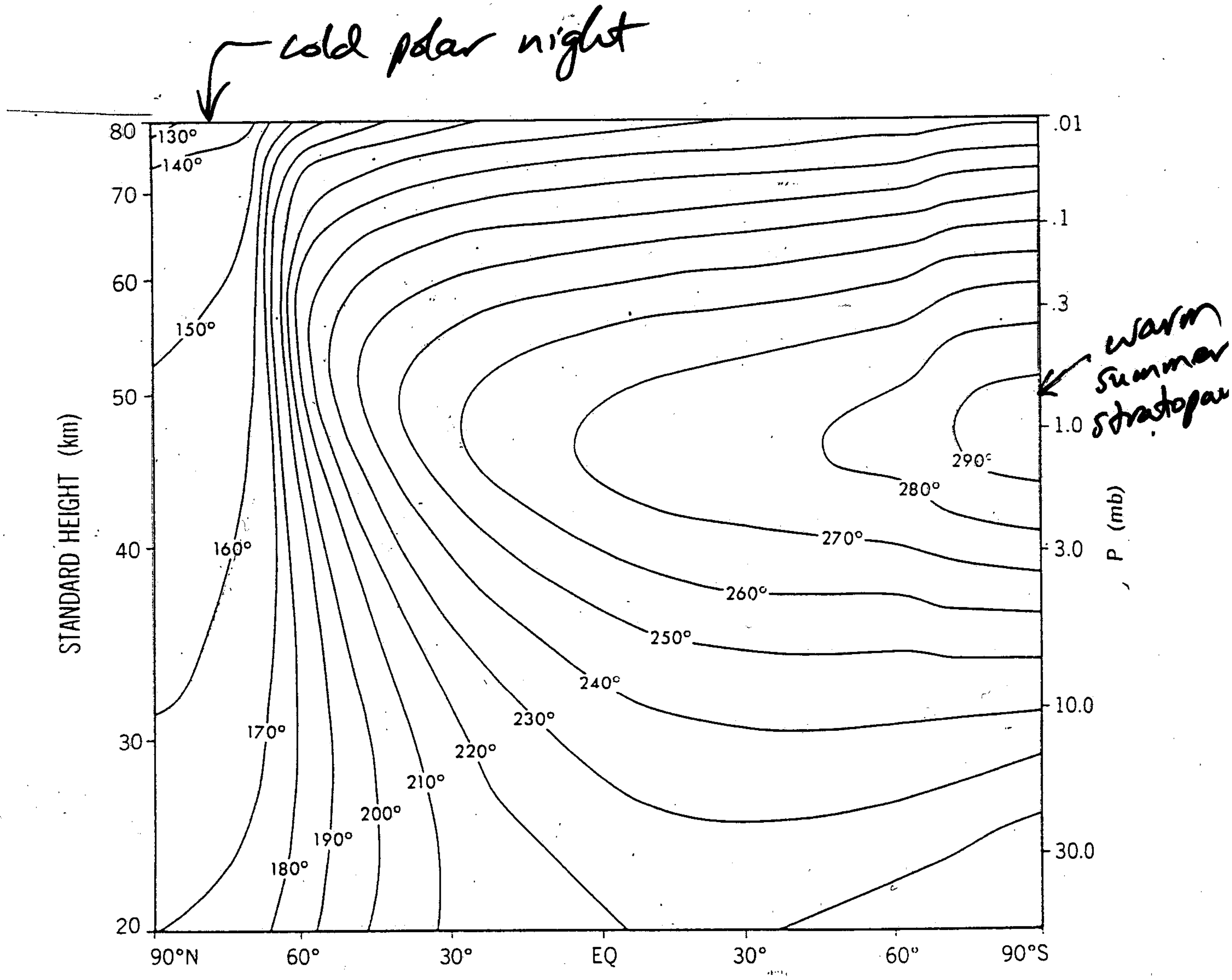

From Fels (1985)

Zonal-mean zonal wind $\bar{u}$ and temperature $\bar{T}$ at solstice

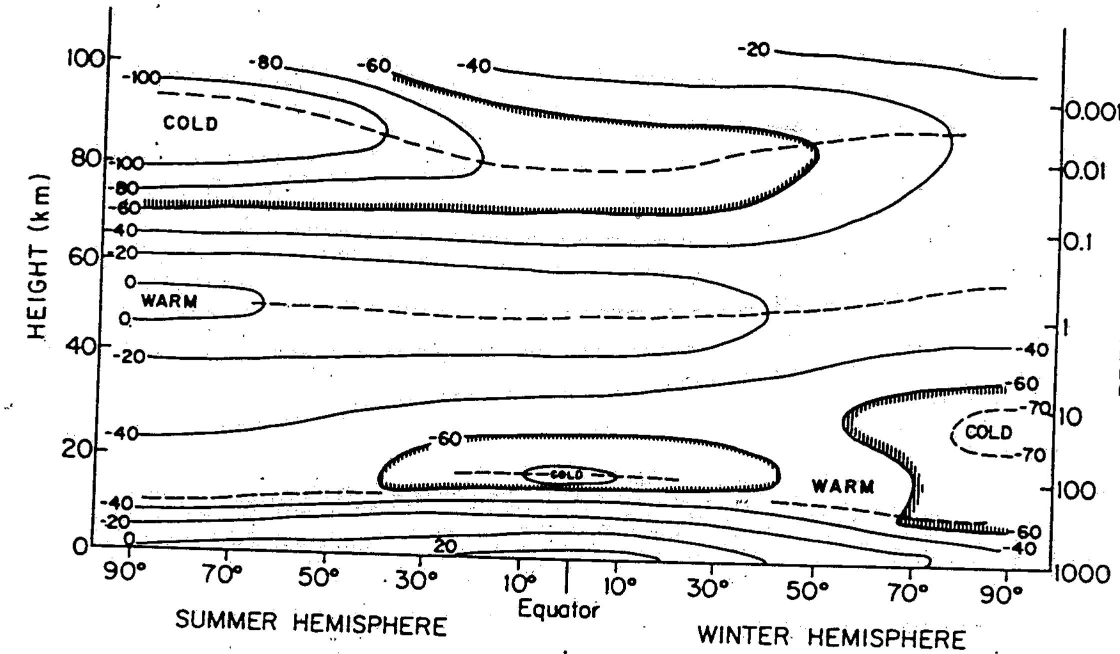

Fig. 1.3. Schematic latitude–height section of zonal mean temperatures (°C) for solstice conditions. Dashed lines indicate tropopause, stratopause, and mesopause levels. (Courtesy of R. J. Reed.)

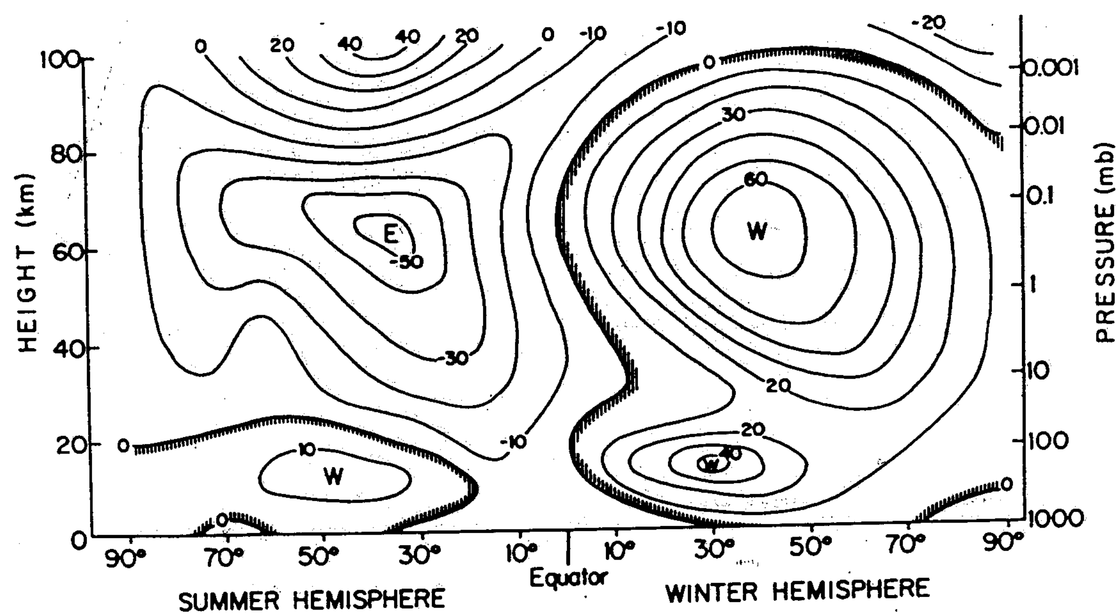

Fig. 1.4. Schematic latitude–height section of zonal mean zonal wind ($m\ s^{-1}$) for solstice conditions; W and E designate centers of westerly (from the west) and easterly (from the east) winds, respectively. (Courtesy of R. J. Reed.)

from Andrews, Holton & Leovy (1987)

Residual (TEM) circulation in Canadian Middle Atmosphere Model (CMAM)

→ Brewer-Dobson circulation

Mass streamlines

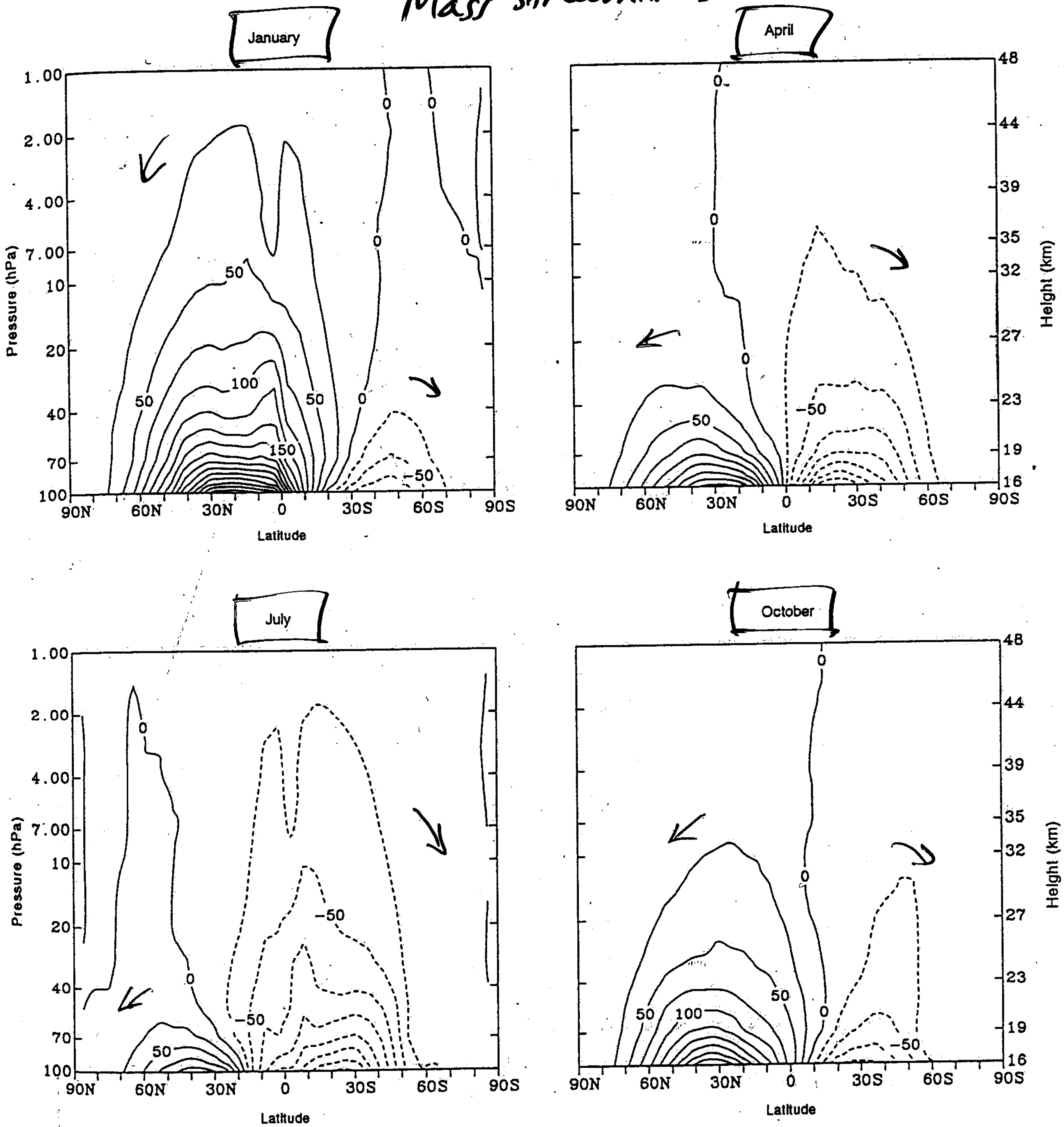

Calculations by John Koshyk, University of Toronto

N_2O from CLAES : Randel et al. 1993 Nature

- tropical upwelling
- extratropical downwelling
- subtropical barrier

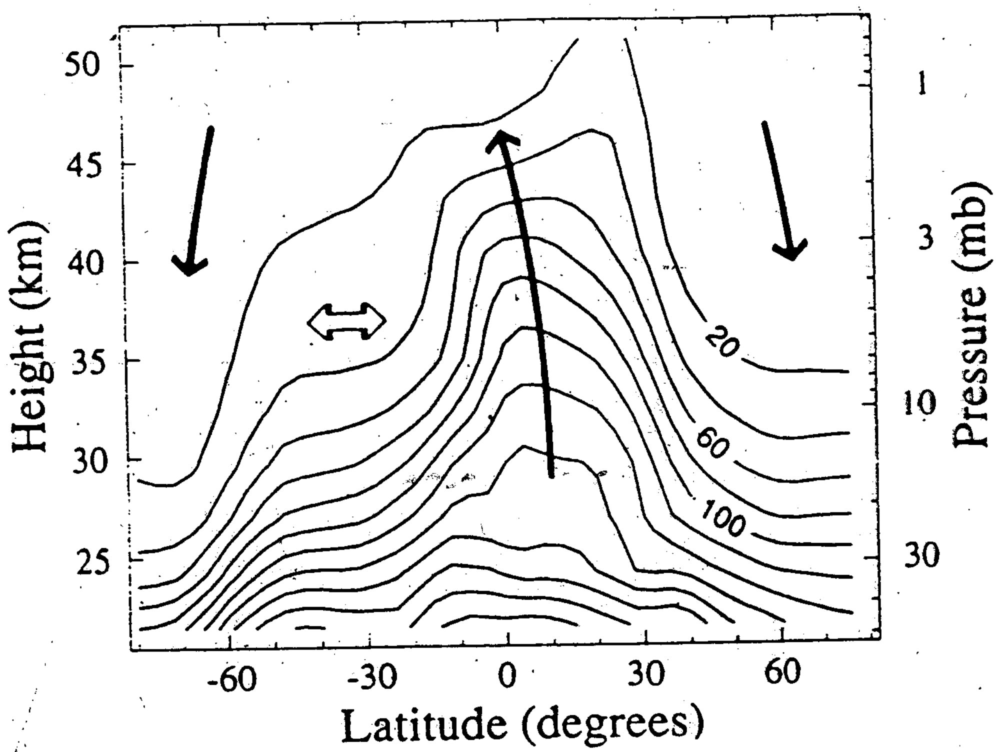

FIG. 1 Longitudinally averaged structure of nitrous oxide (N_2O) mixing ratio (in parts per billion (10^9) by volume (p.p.b.v.)) during 1–20 September 1992 measured by the CLAES instrument on UARS. Heavy solid lines denote the mean stratospheric circulation in the latitude–height plane, and the horizontal arrows denote the location of quasi-horizontal mixing by planetary waves.

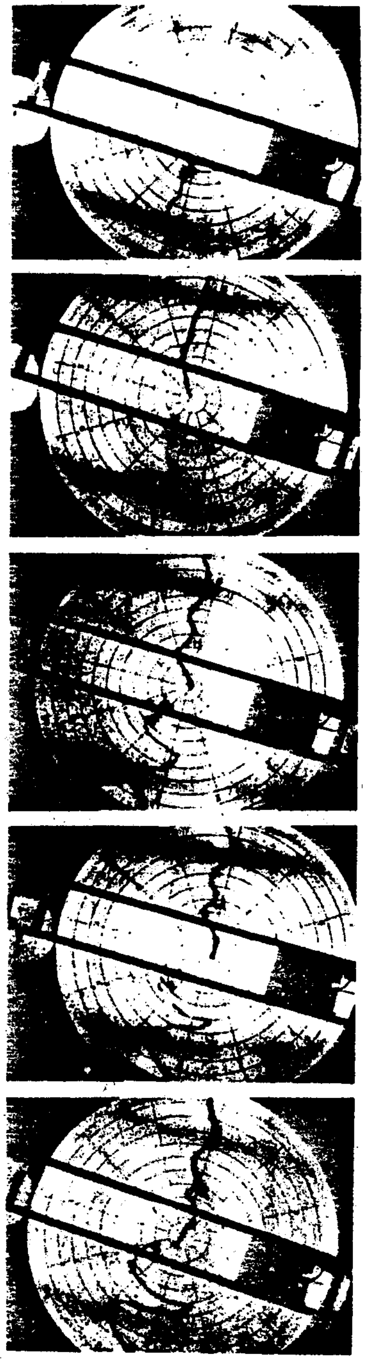

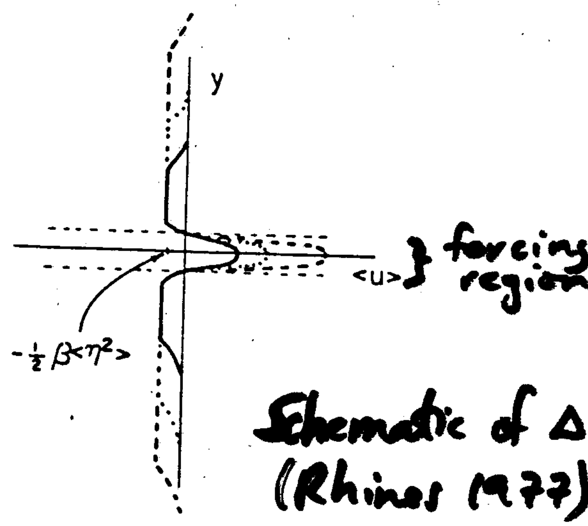

Schematic of $\Delta\bar{u}$
(Rhines 1977)

Fig. 50. Mean circulation induced by an isolated disturbance (beneath the black square) on a polar β plane (Whitehead, 1975). The dye streaks deforming with time show a prograde (eastward) jet at the forcing latitudes, with westward flow elsewhere.

Lab expts. (Whitehead 1975 Tellus)
vertically forced motion

→ Momentum is transferred
up-gradient!

Winds and height contours

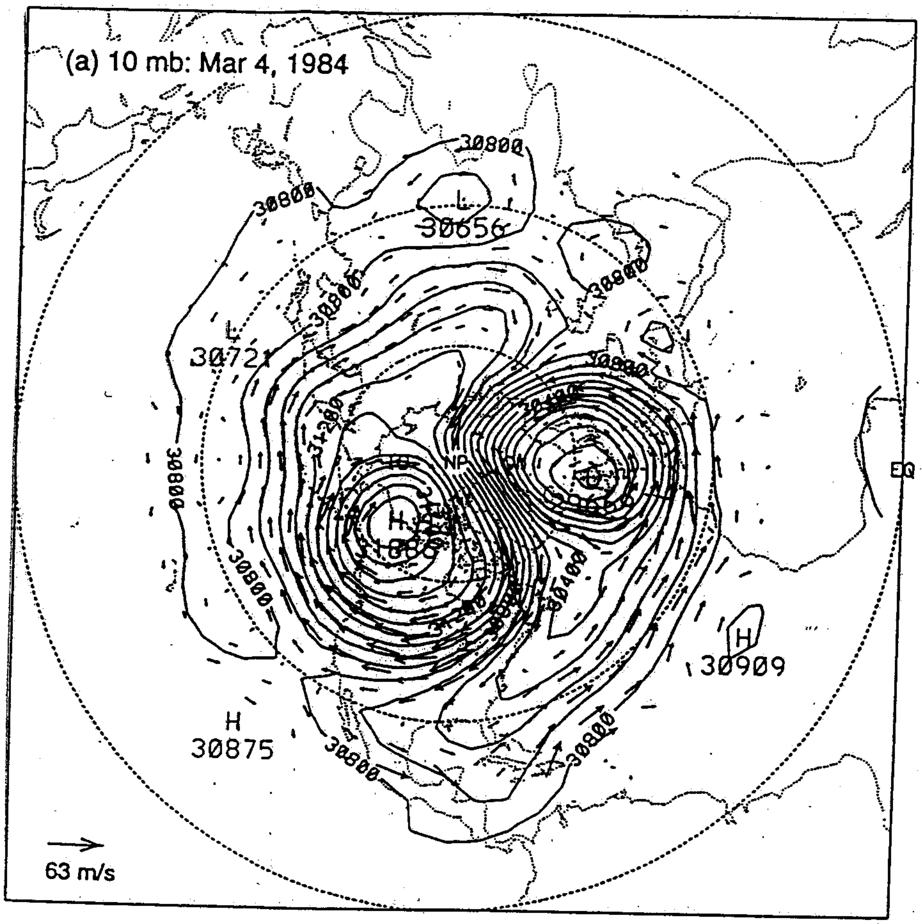

10 mb

~ 35 km

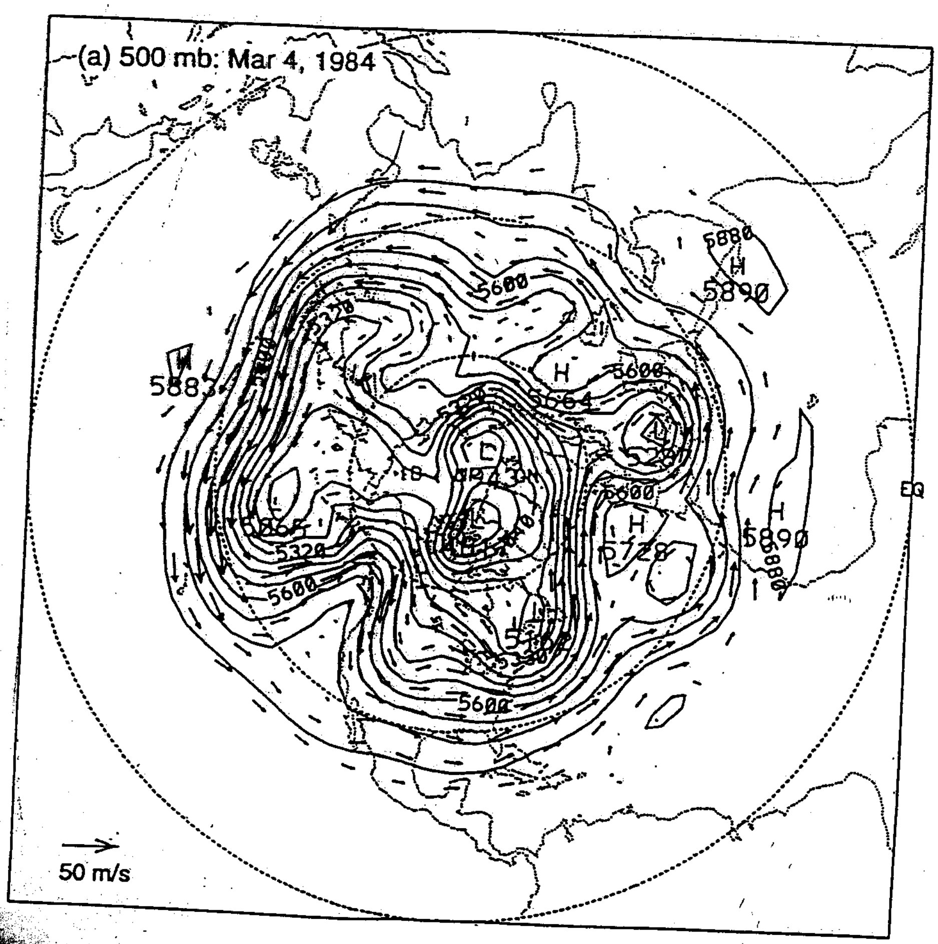

500 mb

~ 5 km

Downward control

<u>Simple thought-experiment</u>: apply localized mechanical forcing in presence of Newtonian cooling and surface drag (take $F < 0$, like Rossby-wave drag)

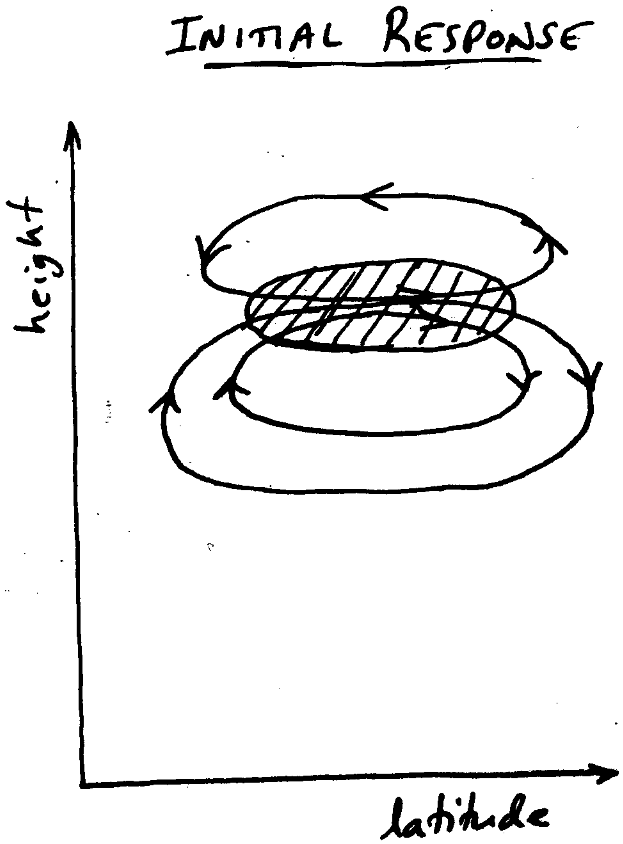

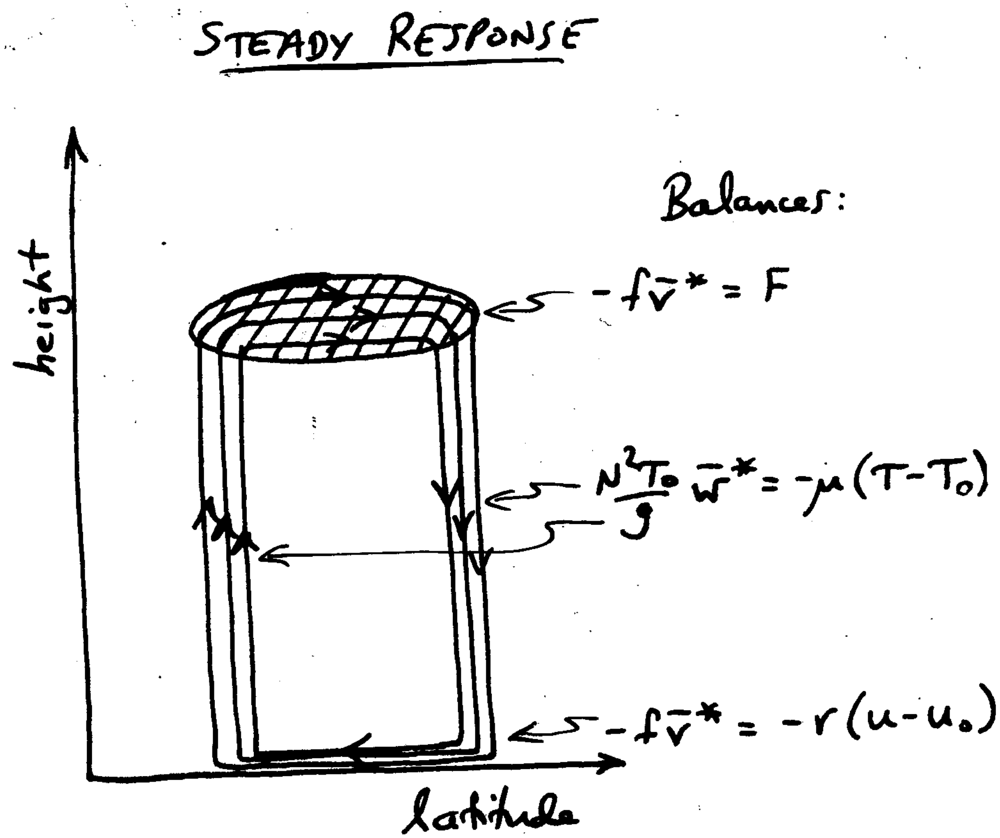

Annual cycle of lower-stratosphere temperature

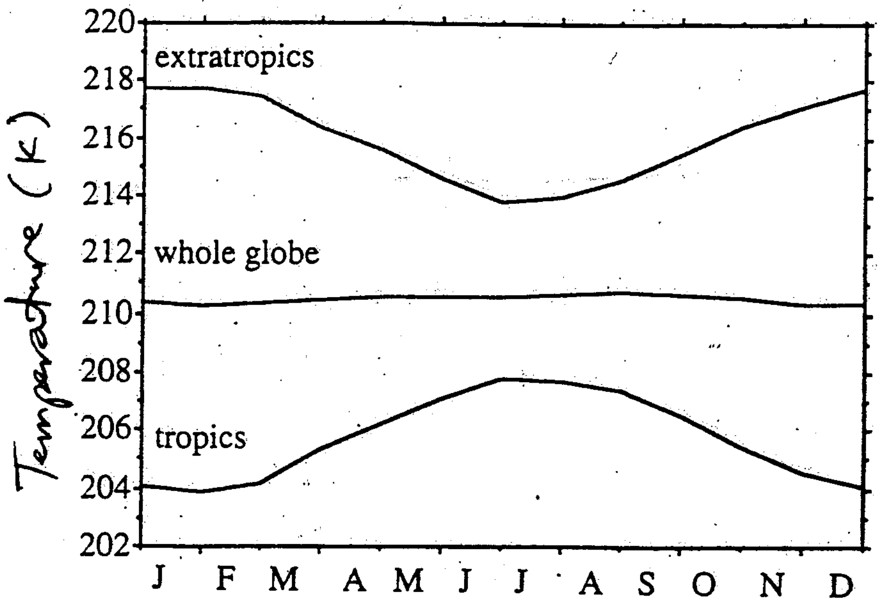

FIG. 2. Climatological mean annual march of lower-stratospheric temperature based on MSU-4 data for the period 1979–91, averaged over the tropics (30°S–30°N), the extratropics (poleward of 30°S and 30°N), and the entire globe.

Yulaeva, Holton & Wallace (JAS, 1994)

→ annual cycle mainly comes from variations in the diabatic circulation

→ NH winter has a stronger diabatic circulation than SH winter

→ Tropics are always colder than radiative equilibrium, most so in NH winter

The tropical "tape recorder"

→ Cold trap temperatures at tropical tropopause get imprinted on water vapour, and carried up

HALOE (2× CH_4) + H_2O (total water)

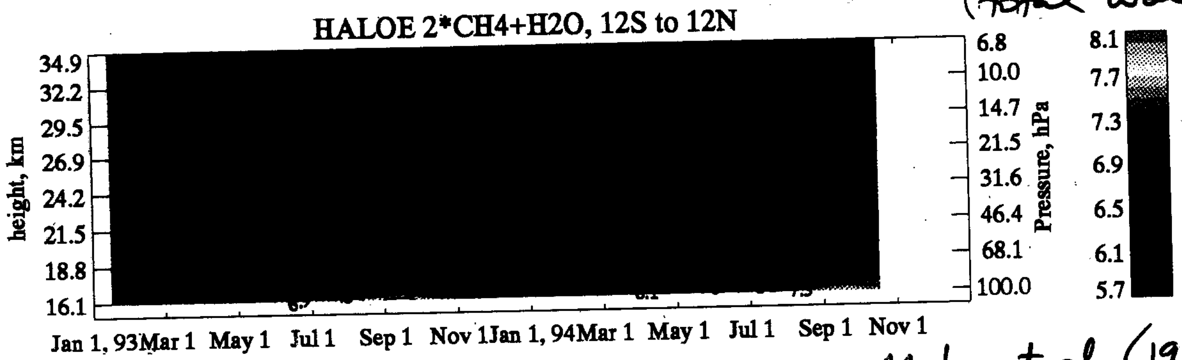

Mote et al. (1996, JGR)

Mote et al. (1996, JGR)

→ Seems to account for otherwise puzzling water vapour profiles measured by ER-2:

Panama: NH summer, 1980

Darwin: NH winter, 1987

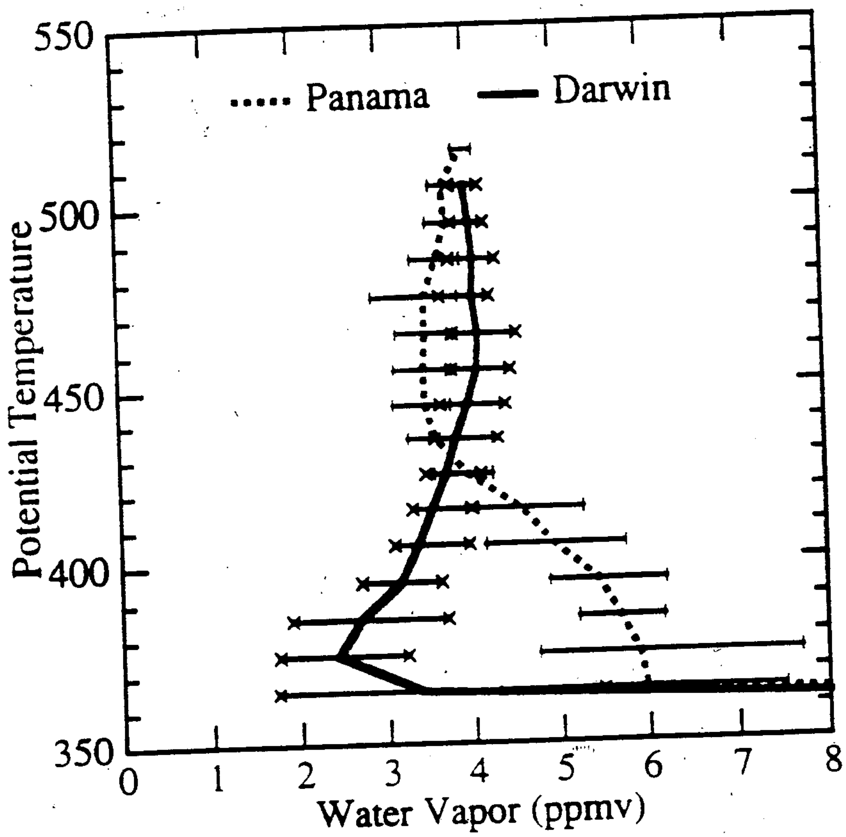

Kelly et al. (1993, JGR)

1993-2002

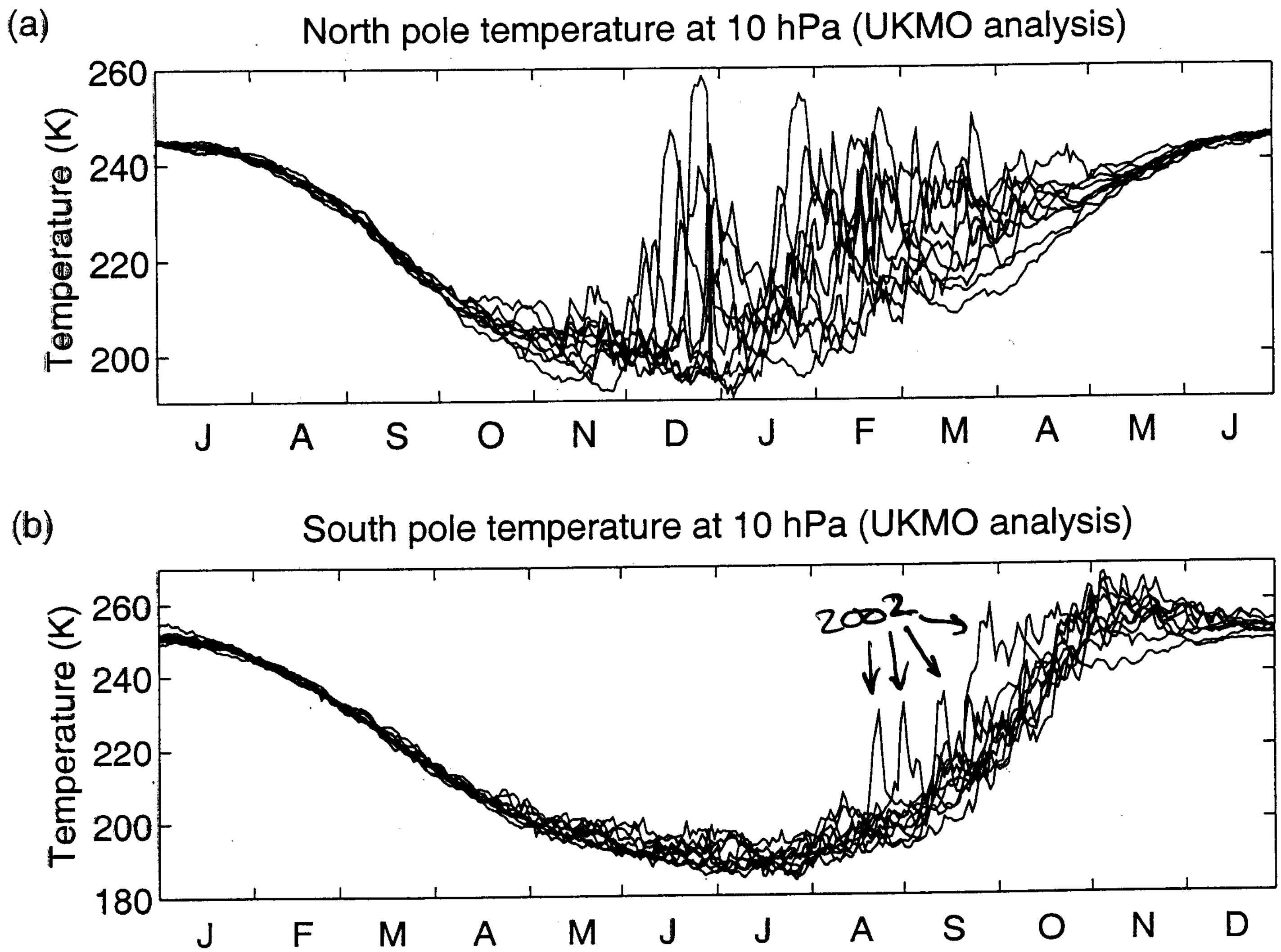

Figure courtesy of Mike Pritchard (University of Toronto)

Distribution of wintertime temperatures (86°N, 2.6 hPa) in millenial integrations with a mechanistic strat-trop PE model

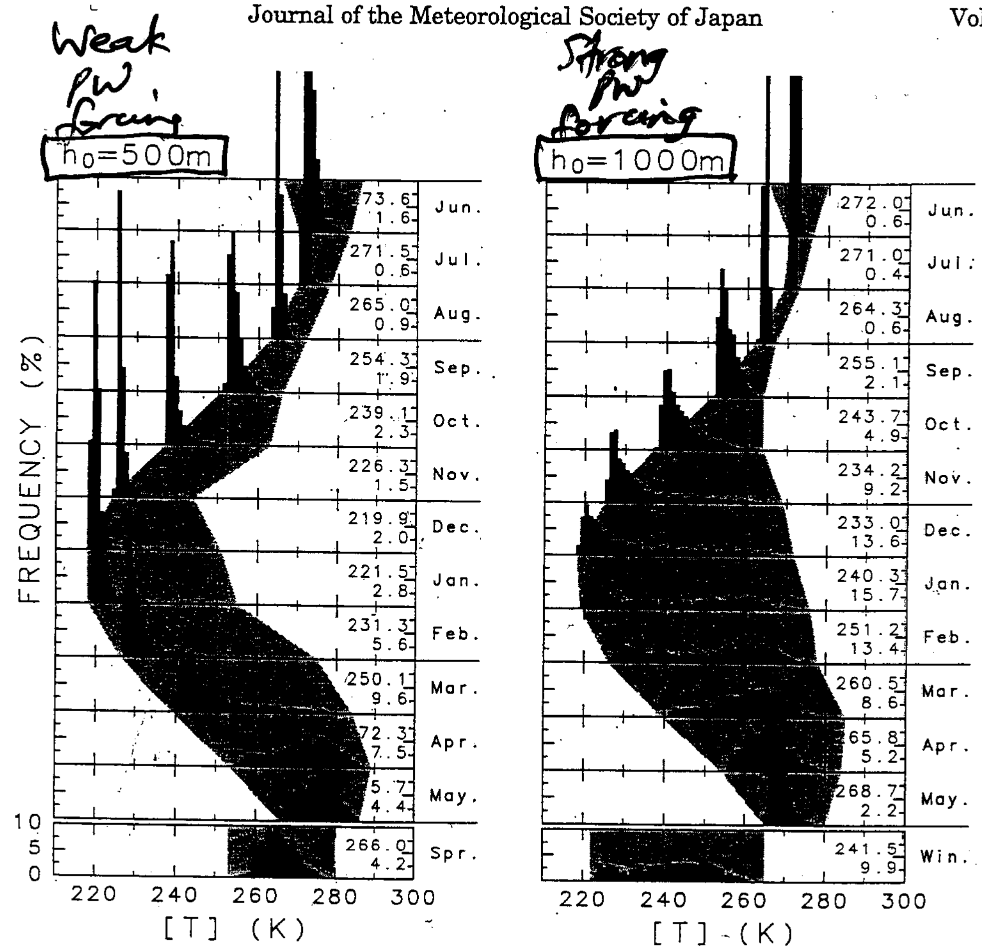

Fig. 10. Frequency distributions of the monthly mean temperature at 86°N and 2.6 hPa for the two millennium integrations: $h_0 = 500$ m (left) and 1000 m (right). Dashed line denotes the 1000-year mean annual variation of the monthly mean temperature, and shade shows the variable range. Averages and standard deviations for the 1000-year data are also written on the right hand side of each panel (top and bottom numbers, respectively). Frequency distributions for a seasonal mean are also displayed in the bottom: spring mean for $h_0 = 500$ m and winter mean for $h_0 = 1000$ m. The downward arrow in the seasonal mean indicates a threshold value for the 200 years of highest temperature.

N.B. Many years are needed to define the PDFs!

Yoden, Taguchi & Naito (2002 JMSJ)

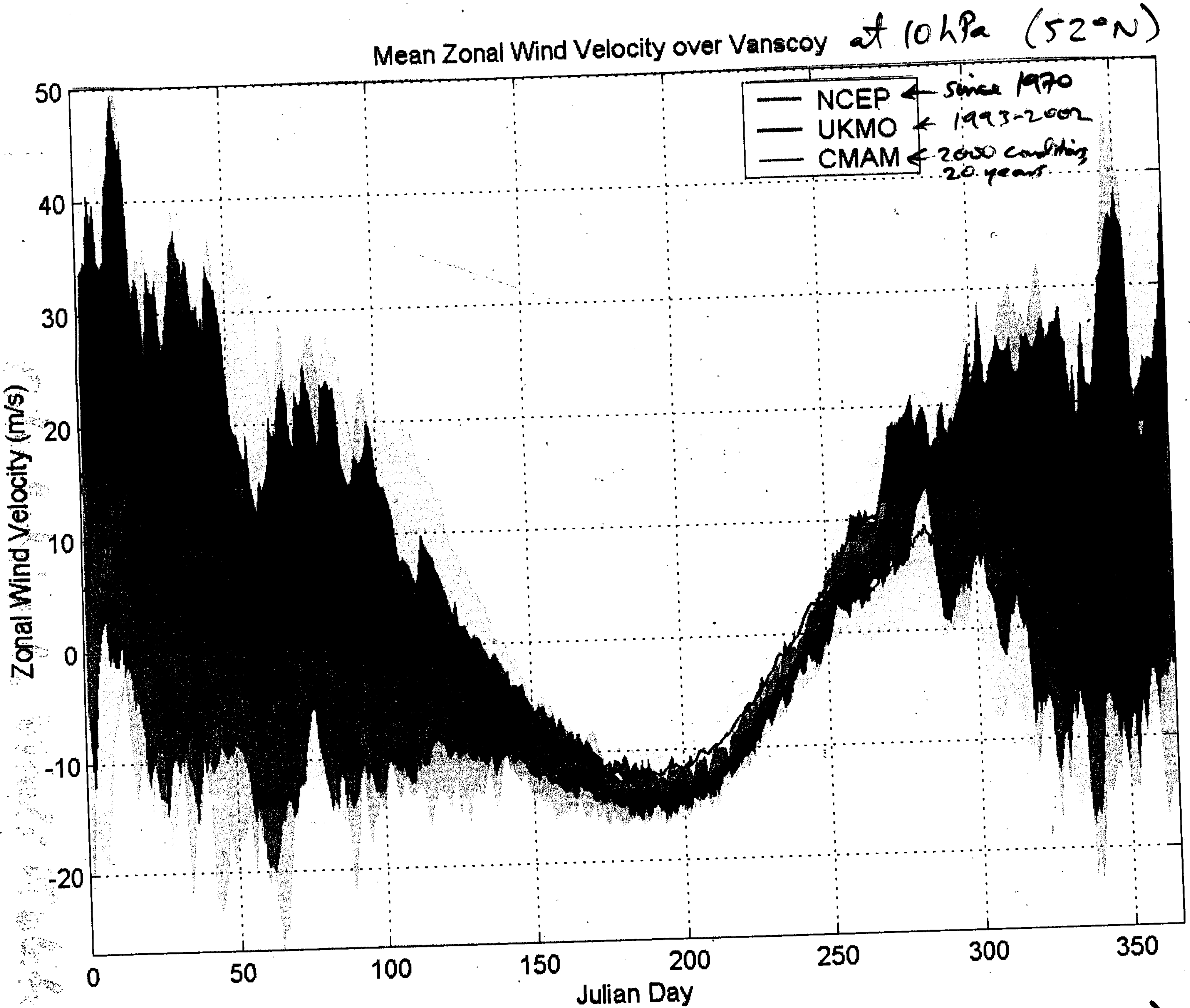

Courtesy of Debra Wunch (University of Toronto)

Balanced response to a negative zonal force

(Boussinesq case)

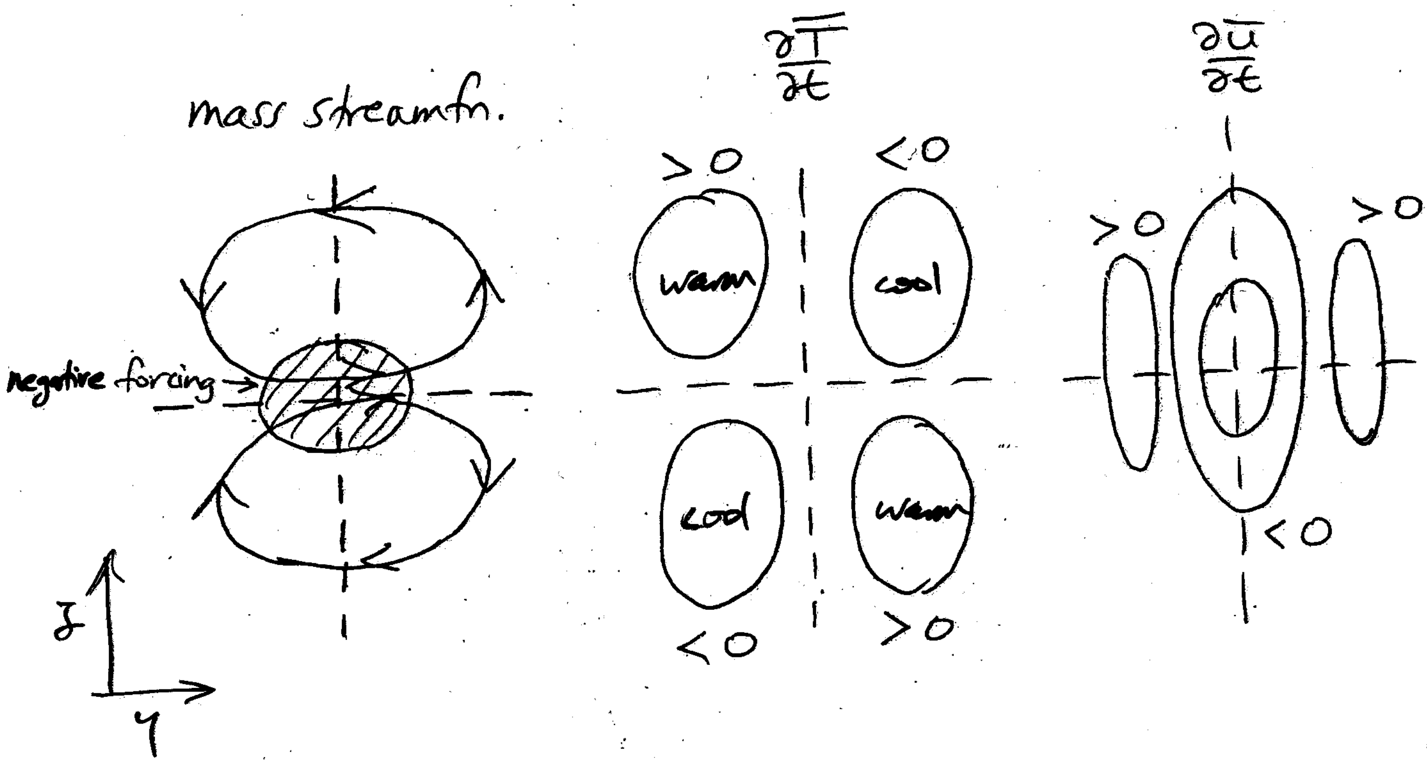

Realistic calculation (spherical, $f_0(z)$)

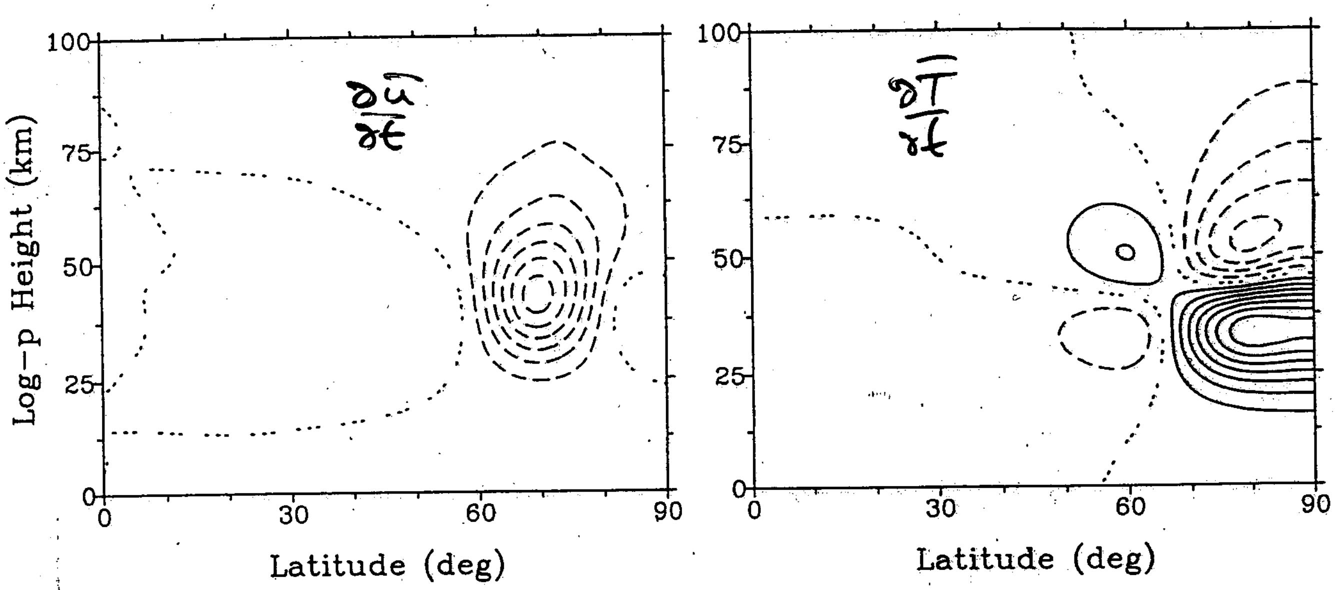

Courtesy of Kirill Semeniuk

Observed evolution of Ertel potential vorticity (polar sterographic projection of Arctic)

FEB 1979 850 K ~ 30 km altitude

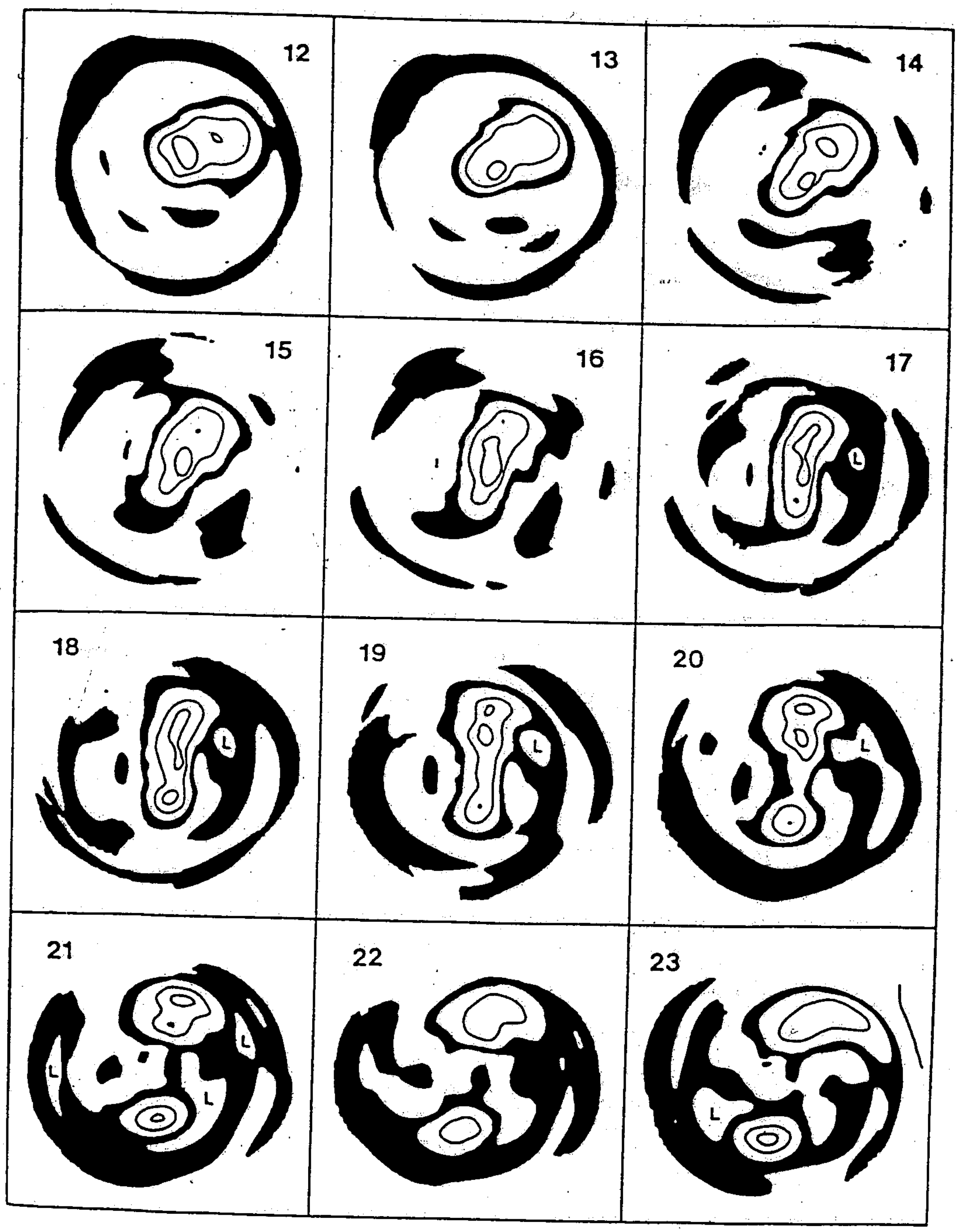

→ A "wave-two" sudden warming

Dunkerton & Delisi (1986 JGR)

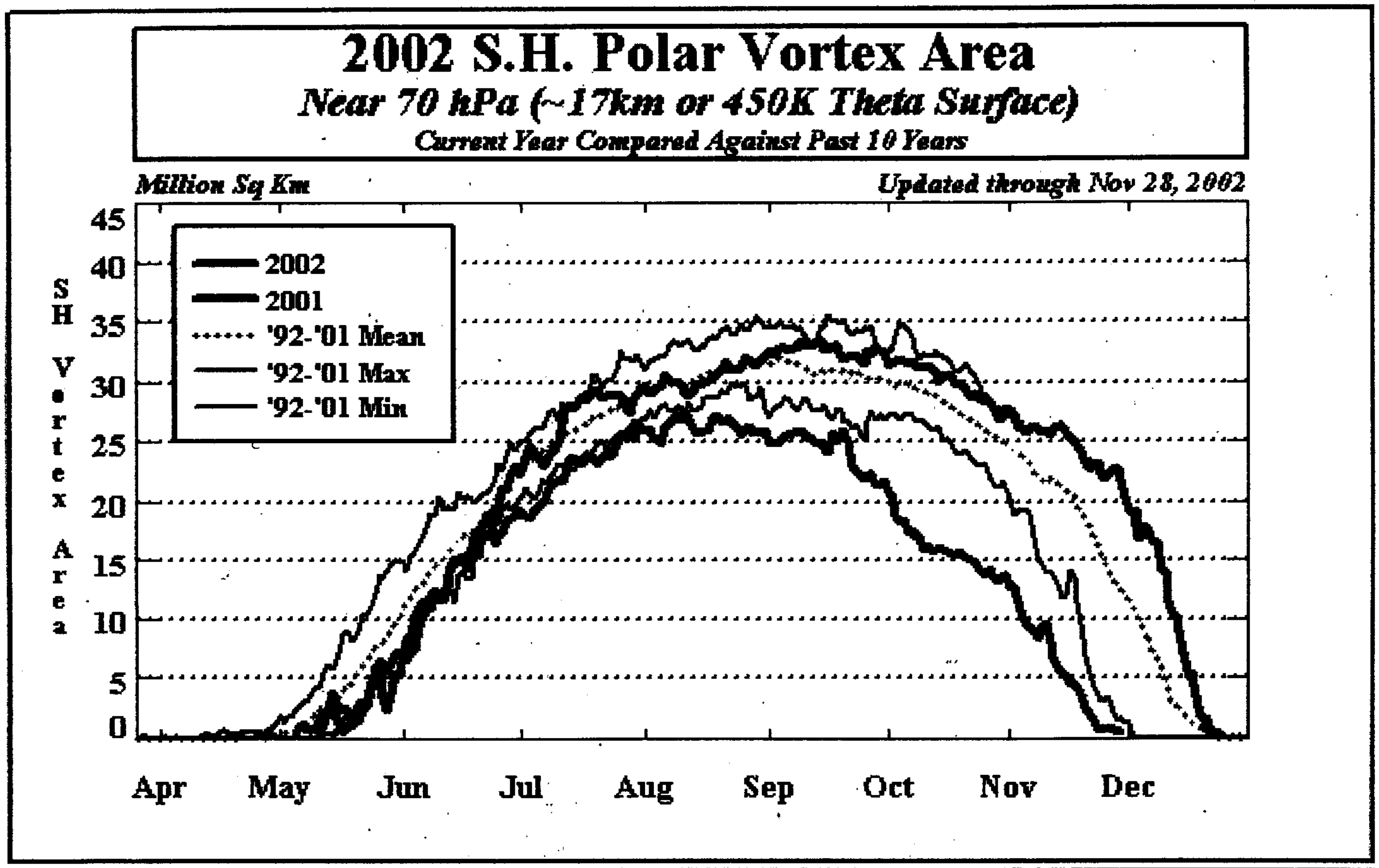
2002 S.H. Polar Vortex Area
Near 70 hPa (~17km or 450K Theta Surface)
Current Year Compared Against Past 10 Years
Million Sq Km
Updated through Nov 28, 2002
SH Vortex Area
45
40
35
30
25
20
15
10
5
0
2002
2001
'92-'01 Mean
'92-'01 Max
'92-'01 Min
Apr
May
Jun
Jul
Aug
Sep
Oct
Nov
Dec

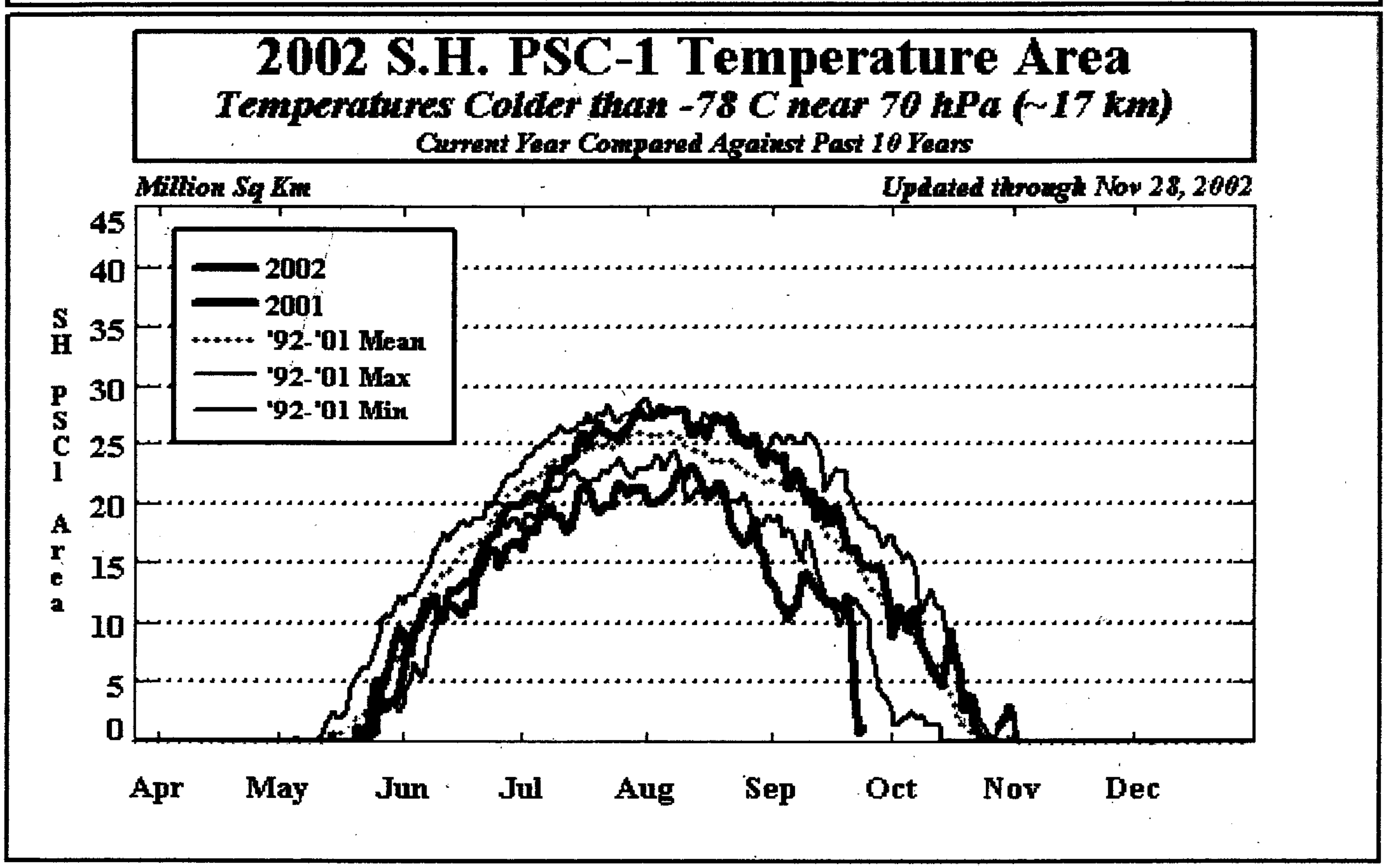
2002 S.H. PSC-1 Temperature Area
Temperatures Colder than -78 C near 70 hPa (~17 km)
Current Year Compared Against Past 10 Years
Million Sq Km
Updated through Nov 28, 2002
SH PSC1 Area
45
40
35
30
25
20
15
10
5
0
2002
2001
'92-'01 Mean
'92-'01 Max
'92-'01 Min
Apr
May
Jun
Jul
Aug
Sep
Oct
Nov
Dec

EP/TOMS Total Ozone for Sep 24, 2002

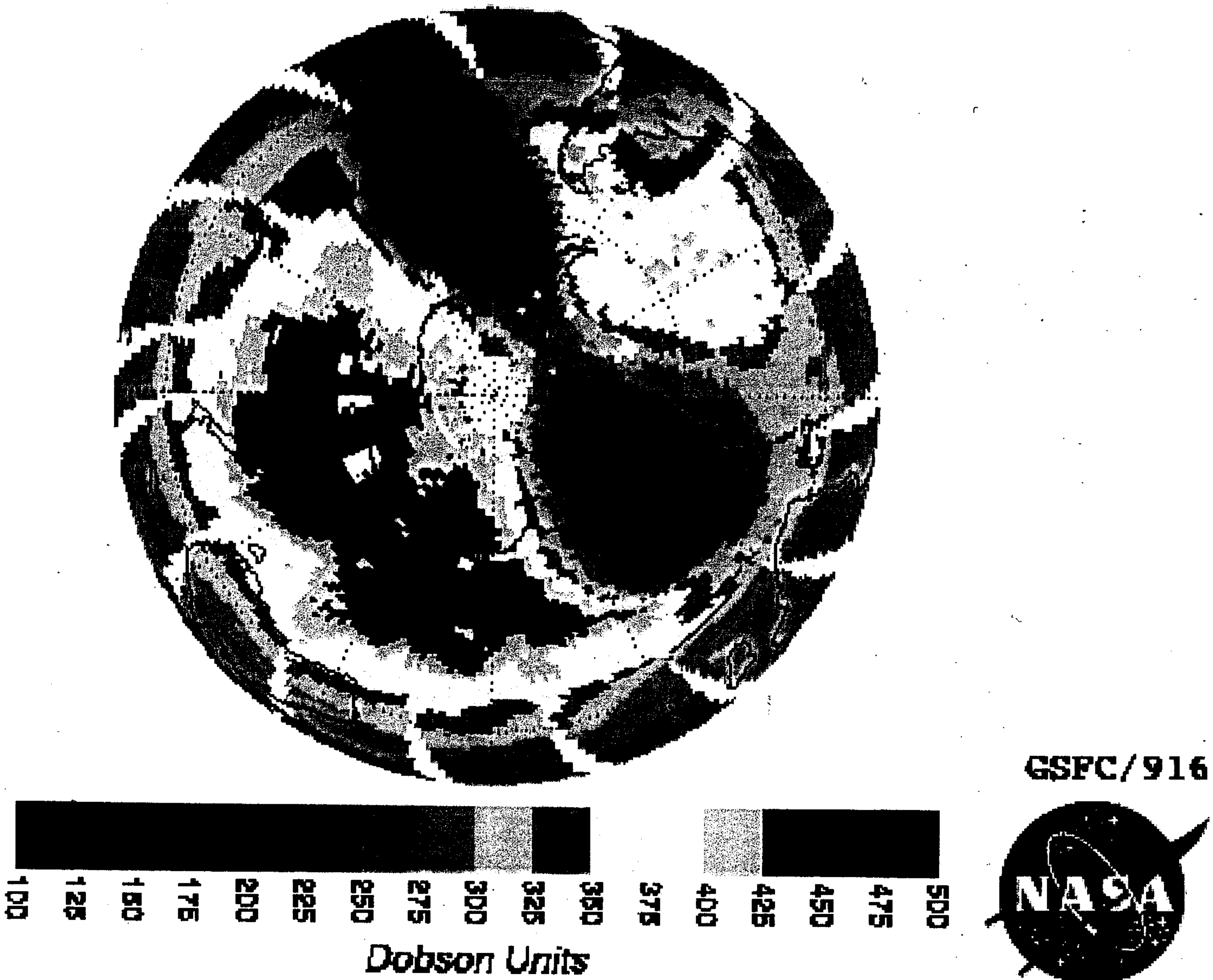

GEN:269:2002

PEMWEST-B

Latitudinal Ozone Distribution Over Western Pacific

Courtesy of E.V. Browell (NASA Langley)

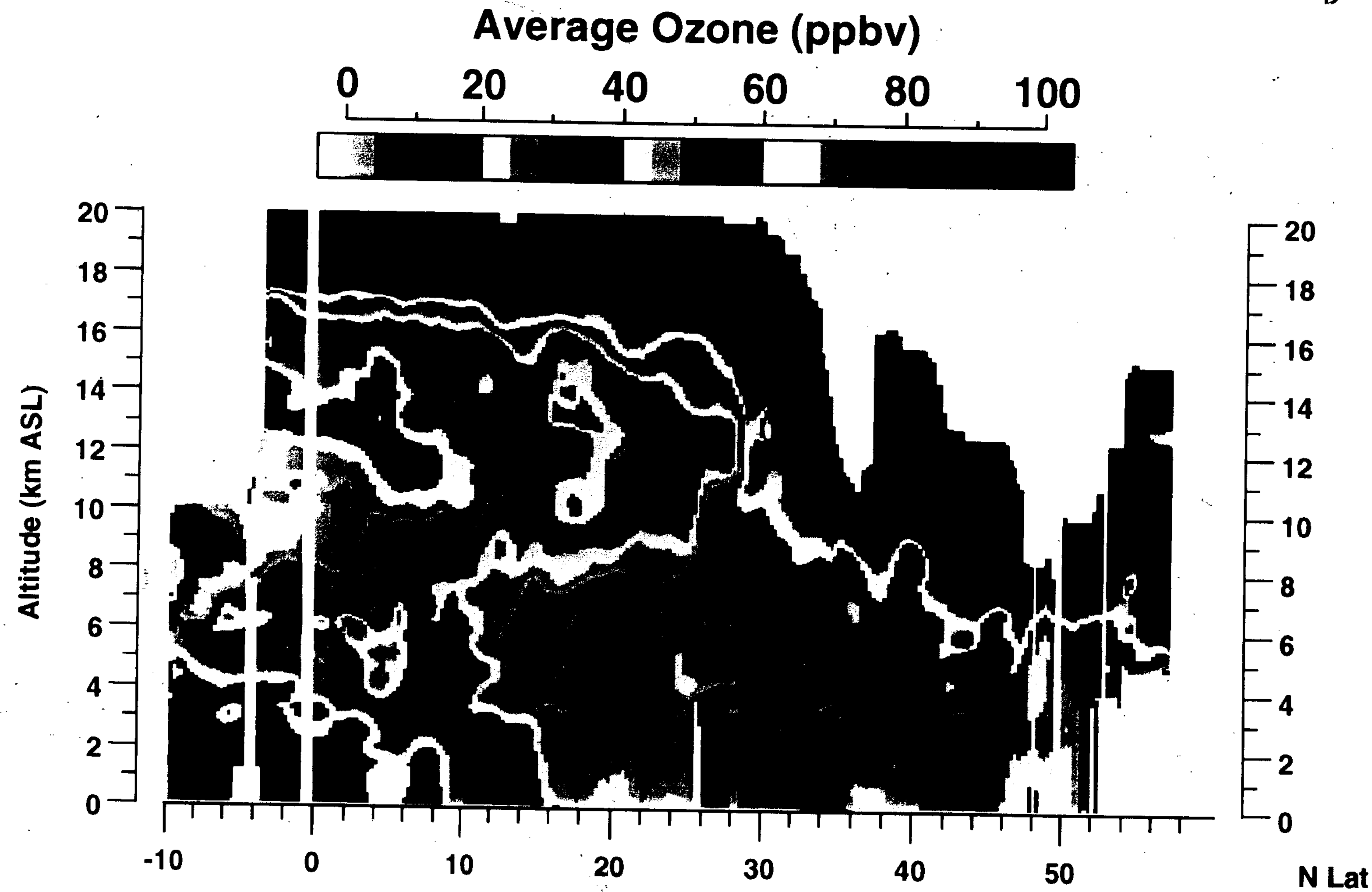

(5JUN95MBC)

Meridional gradient of the mode and mean of the PDF of N_2O on $\Theta = 320$ K from CMAM

(January)

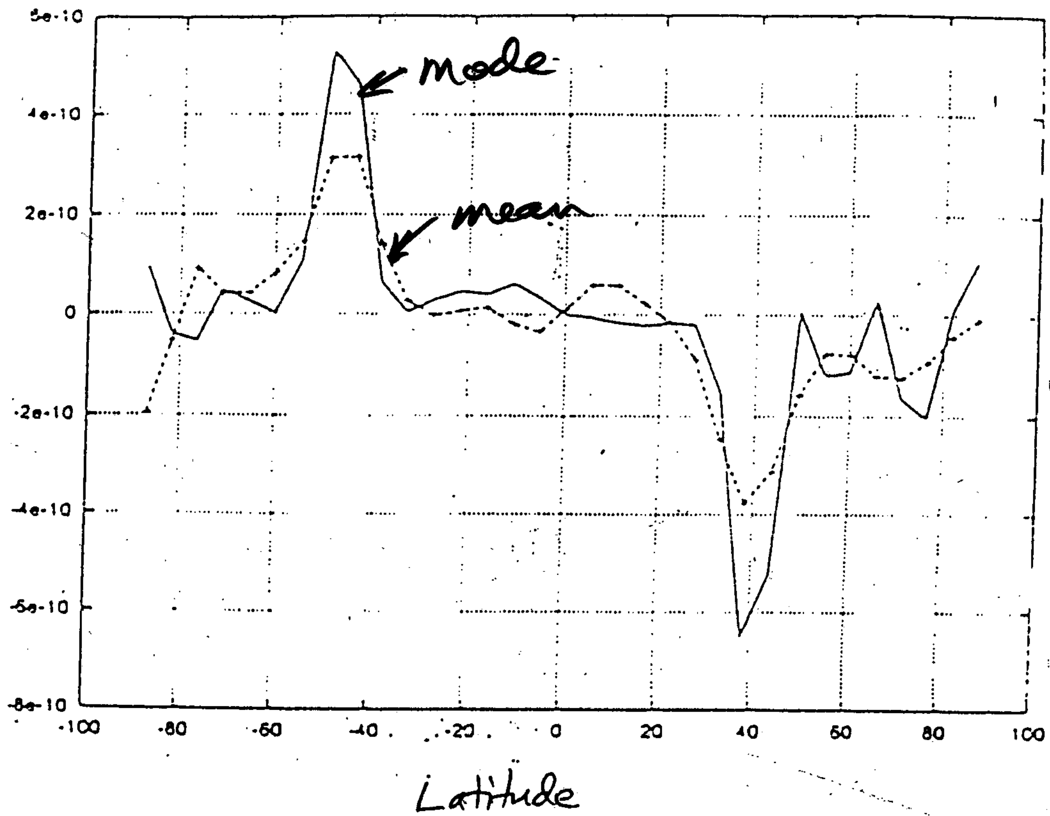

Shows extratropical tropopause in both hemispheres

See Shepherd 2002 JMSJ

After Sparling (2000, Revs. Geophys.)

Calculations by Sunny Arkani-Hamed
University of Toronto

Spatial distribution of N_2O in the stratosphere

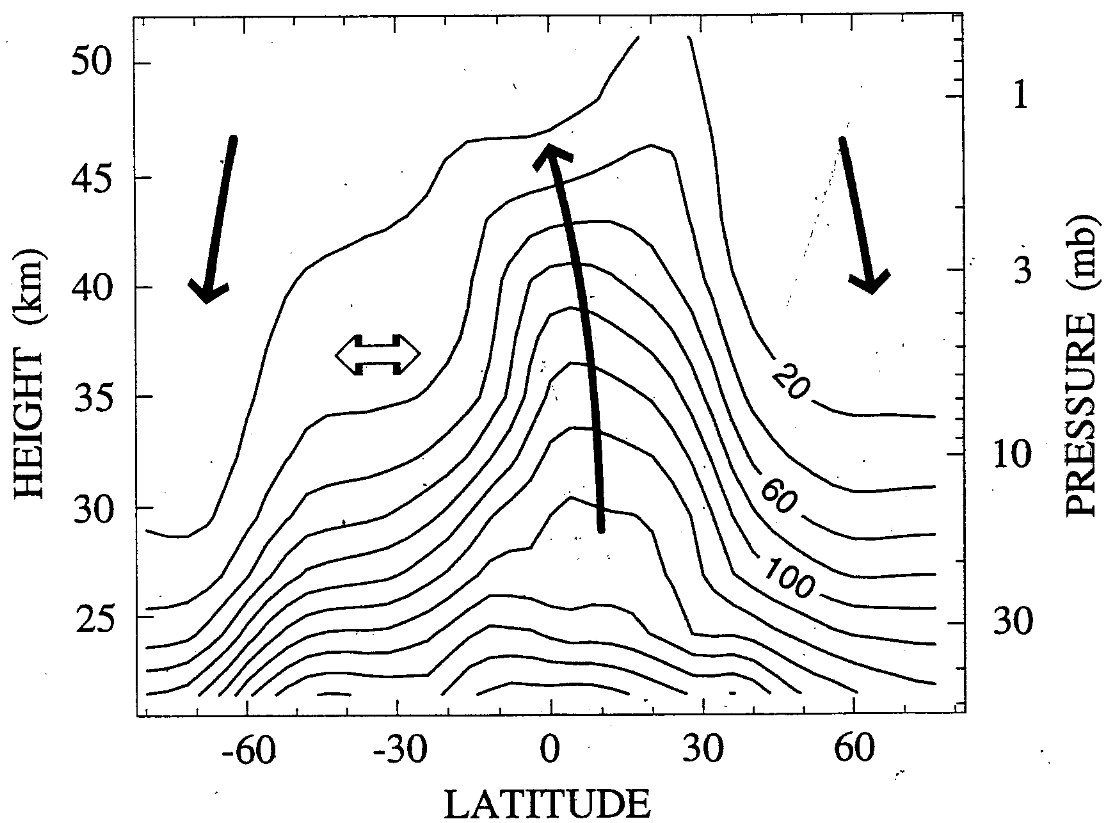

- Upwelling in tropics
- Downwelling in extratropics
- Midlatitude "surf zone" in winter hemisphere

Randel et al. (1993 *Nature*)

Circulation timescales in the stratosphere

"Age" of air relative to tropical tropopause based on advection by diabatic circulation (no mixing!)

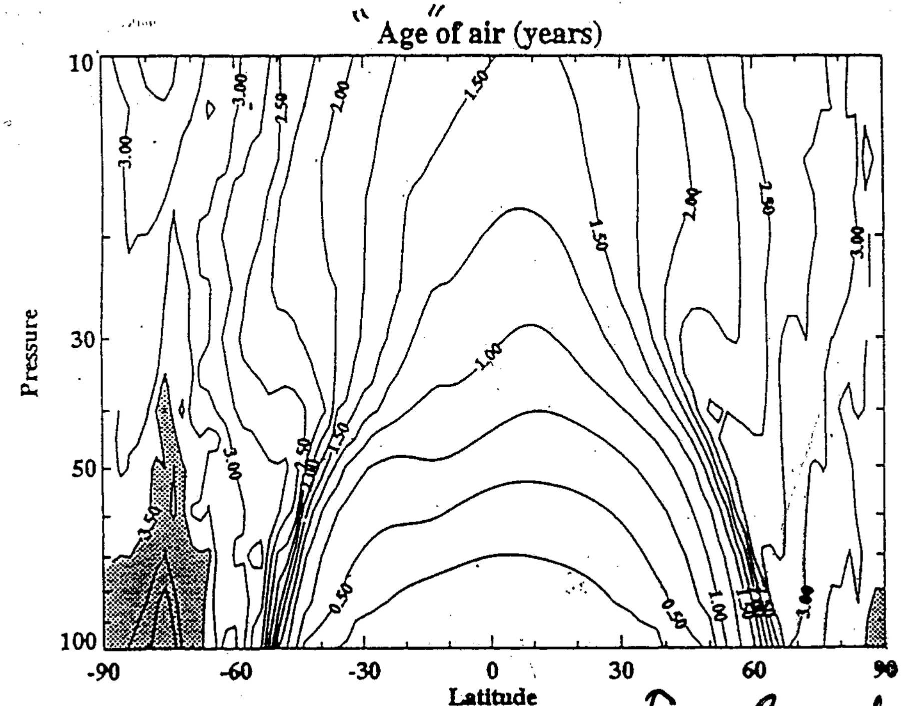

from Rosenlof (1995 JGR)

Mean age of air relative to tropical tropopause in October, from a 3-D CTM

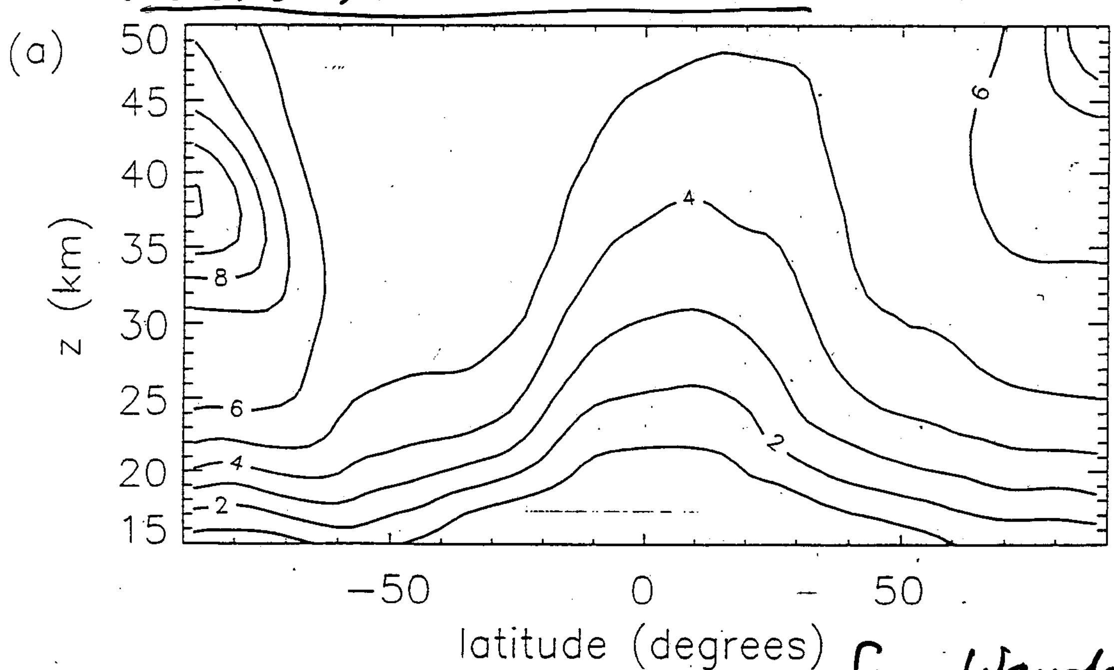

from Waugh et al. (1997 JGR)

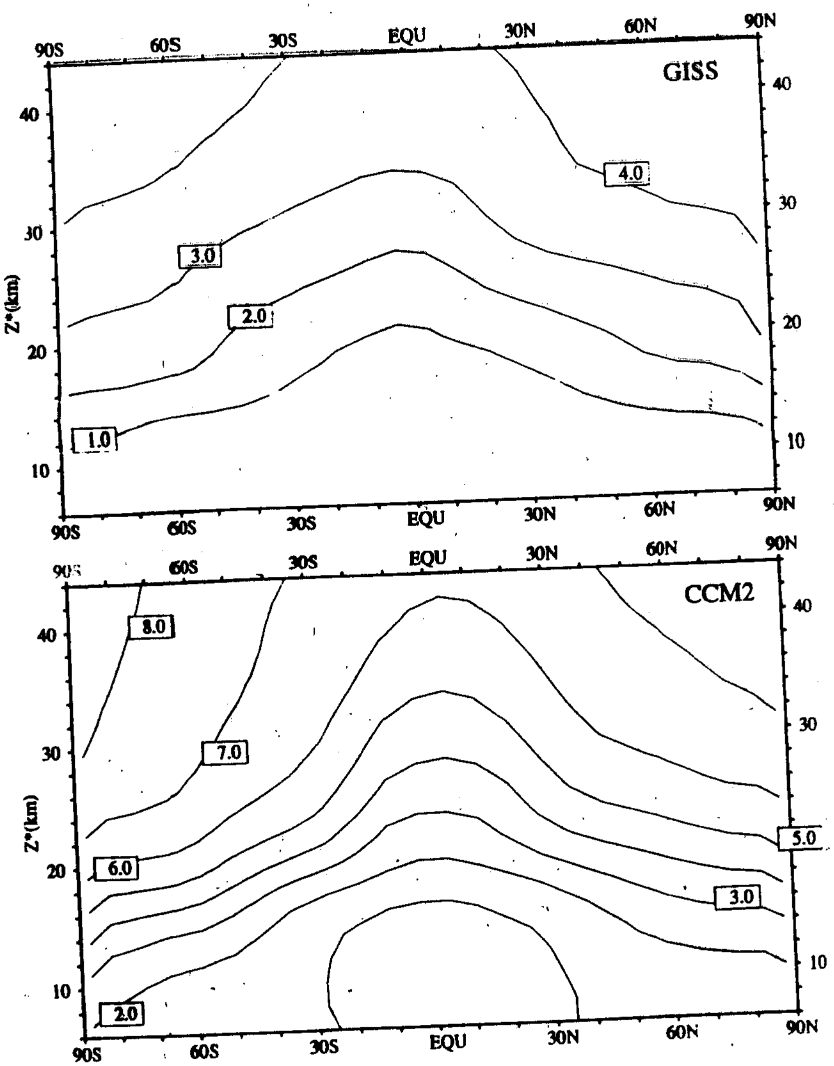

Mean age in two GCMs (in years)

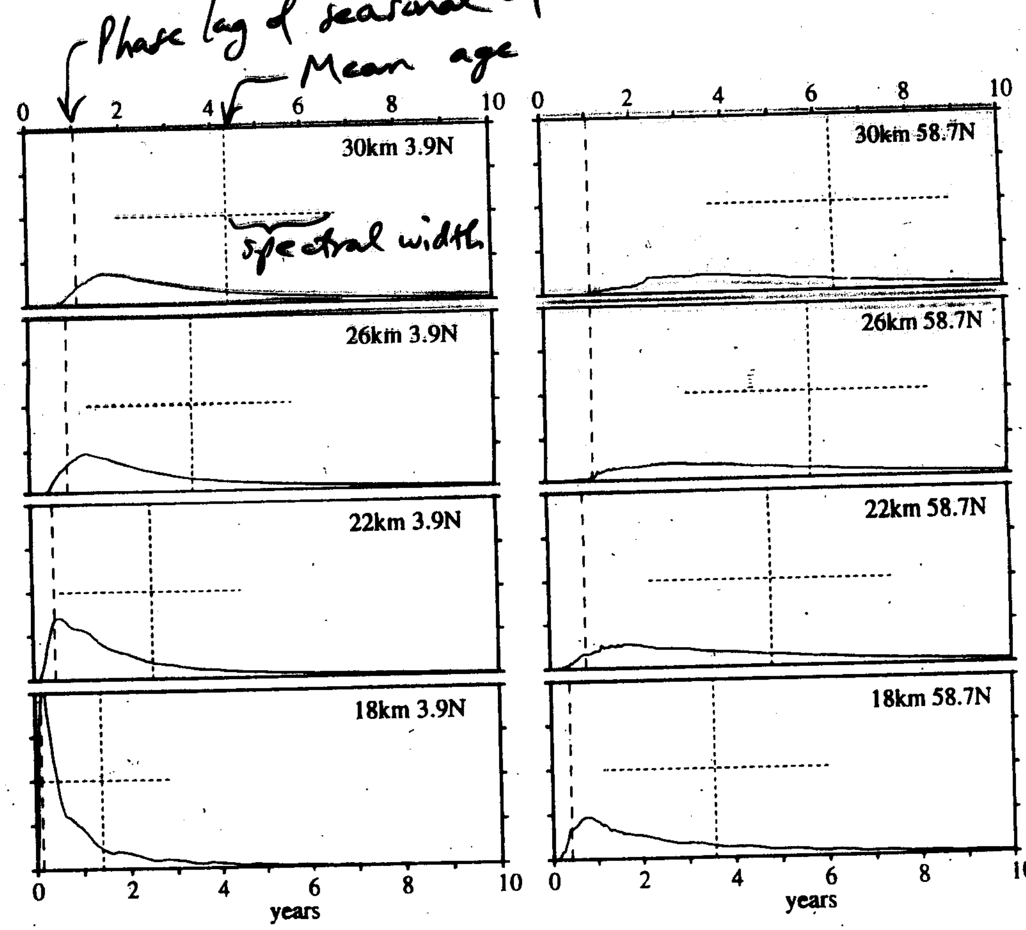

Age spectrum at various locations in CCM2

from Hall & Waugh (JGR 1997)

Breaking planetary waves in the stratosphere

Fig. 8.8. Isopleths of Ertel potential vorticity on an isentropic surface (potential temperature 850 K) near 30 km altitude for 7 December 1981 computed from temperature data from the Stratospheric Sounding Unit on the NOAA 7 satellite (§ 12.8). Units are $Km^2 kg^{-1} s^{-1} \times 10^{-4}$. The shaded region has values between 4 and 6 units. Arrows show the geostrophic flow. The structure of the planetary wave suggests that it is 'breaking'. (After Clough *et al.*, 1985)

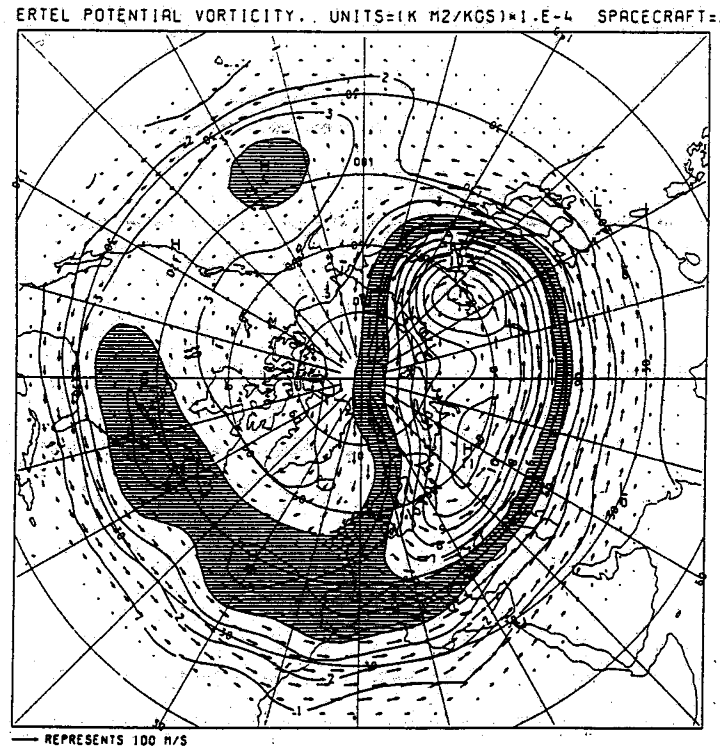

Potential vorticity (polar stereographic view) on 850 K isentropic surface (near 30 km altitude) derived from satellite measurements

→ Breaking wave-1

from Houghton (1986)

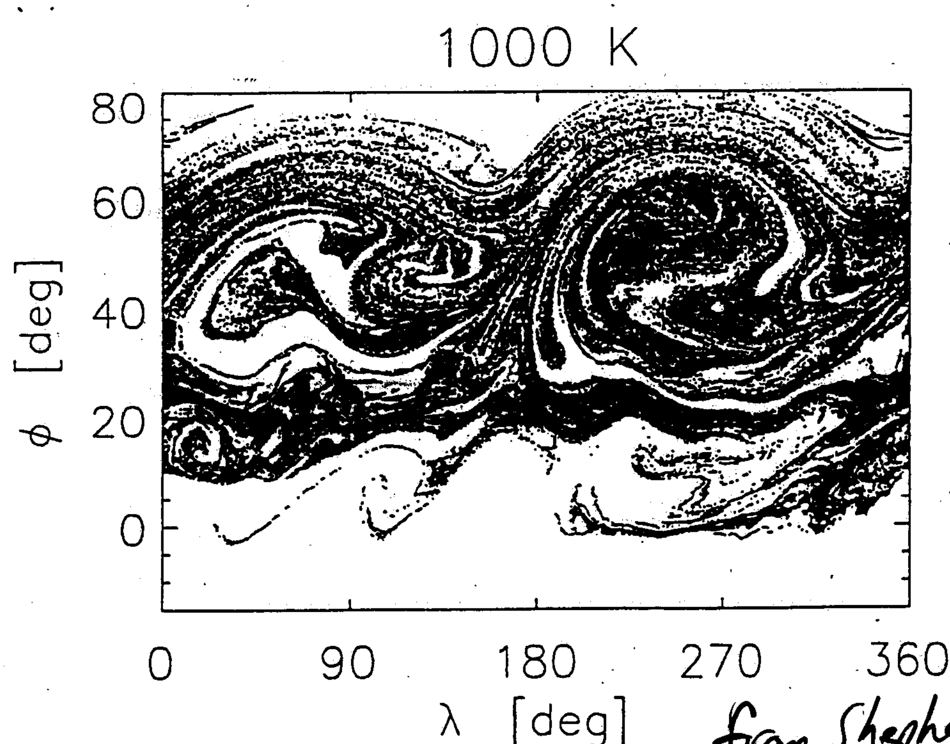

Particle advection from CMAM-GCM winds on 1000K isentropic surface (near 35 km alt.)

→ Breaking wave-2

from Shepherd, Koshyk & Ngan (2000, JGR)

Courtesy of E.V. Browell (NASA Langley)

TAHITI TO AMES
FLIGHT 9

AASE 2 **30 JAN 92**

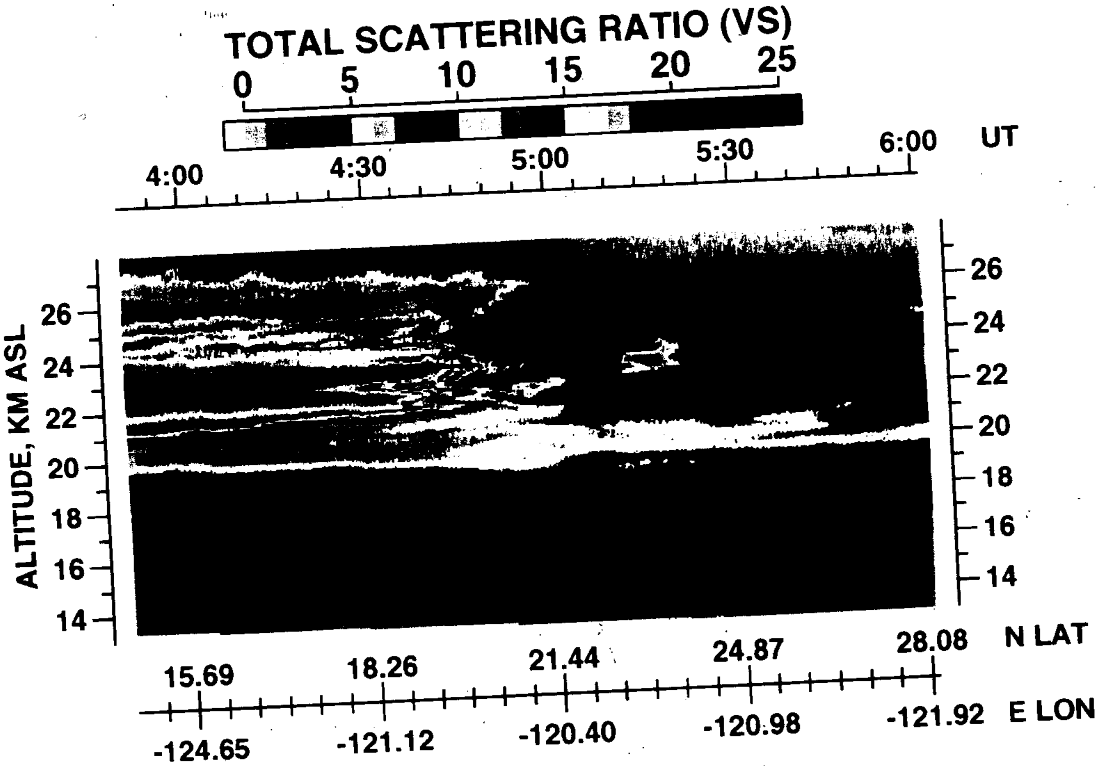

Published in Grant et al. JGR (1994)

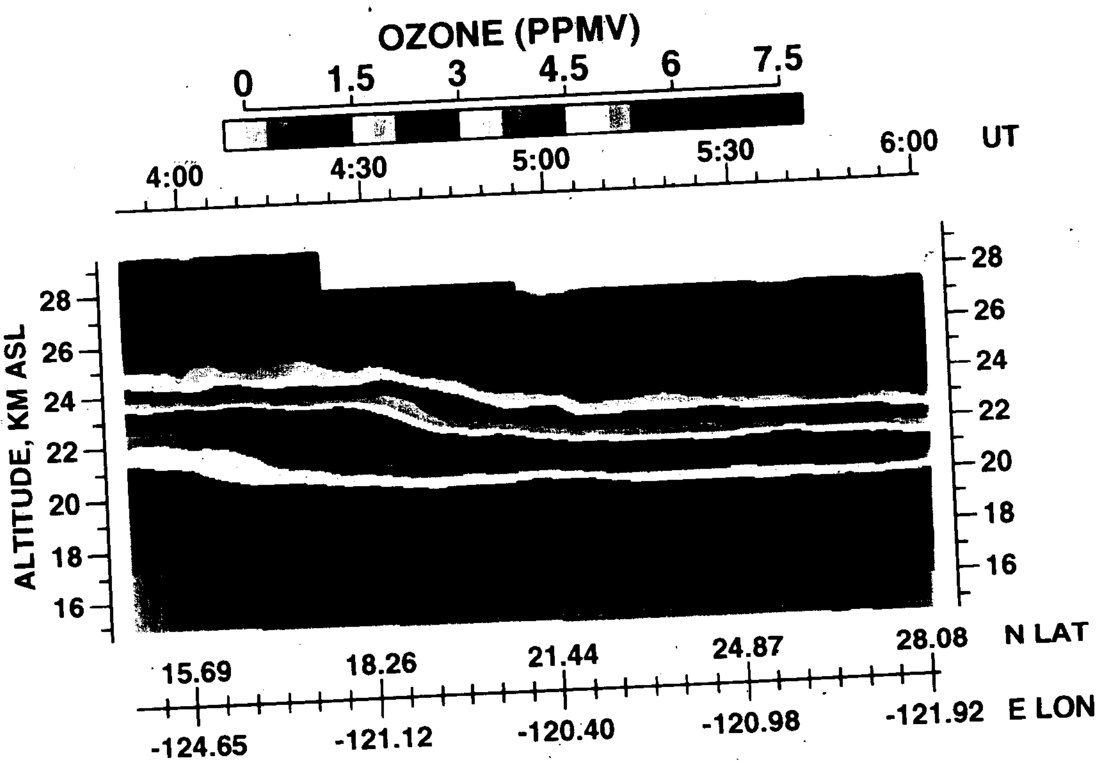

#5

Evolution of passive tracer particles in lower stratosphere during SH winter, from CMAM.

- Isentropic winds on 450 K surface (≈ 17 km)
- Evolution from 1 to 30 July

Initial distribution

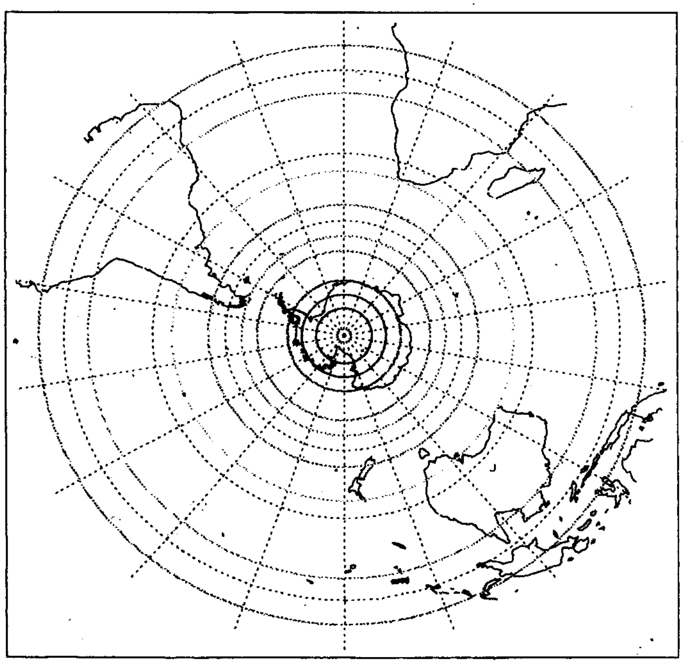

Distribution after 30 days

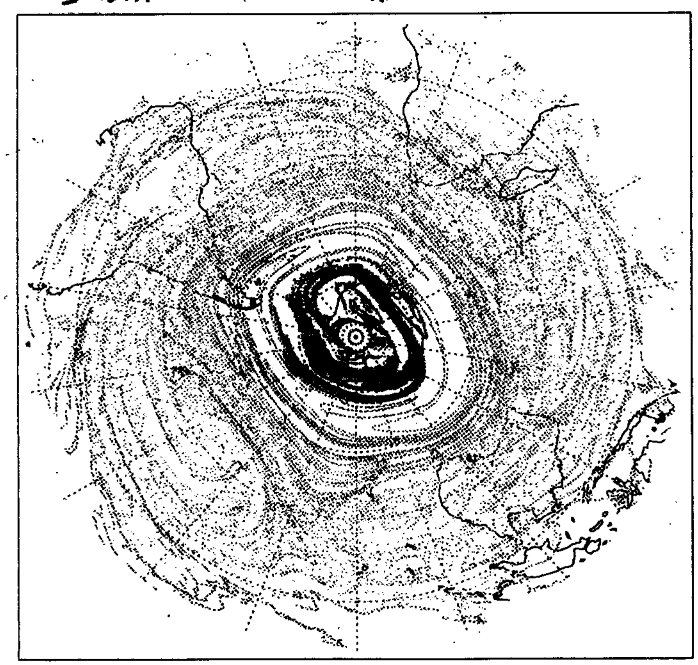

Courtesy of Keith Ngan, University of Toronto

Transport and mixing in the lower stratosphere

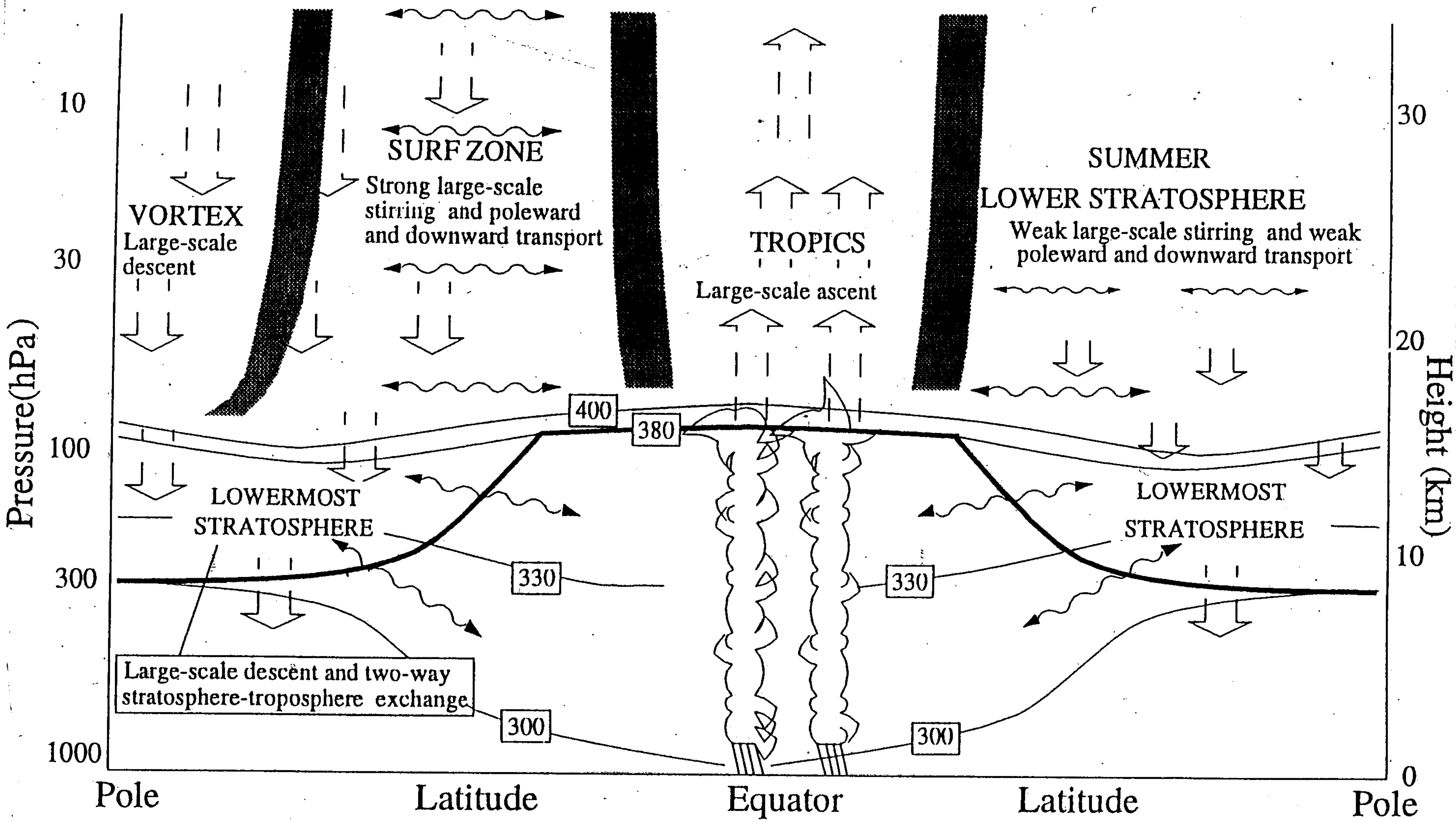

Composed by Peter Haynes et al.
Chapter 7 of WMO:1998

Observed changes in total ozone over past decades

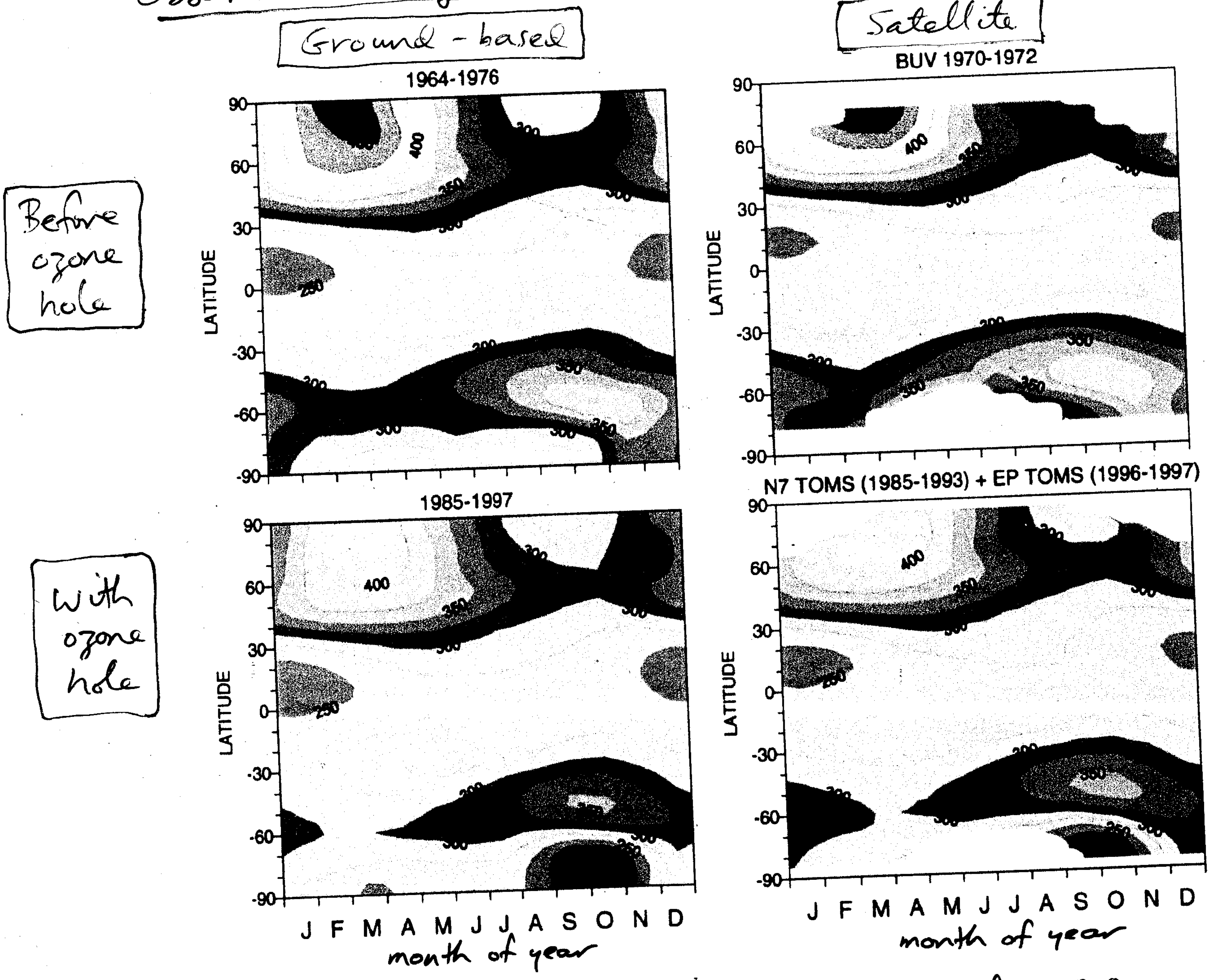

from Chapter 4 of 1998 Ozone Assessment

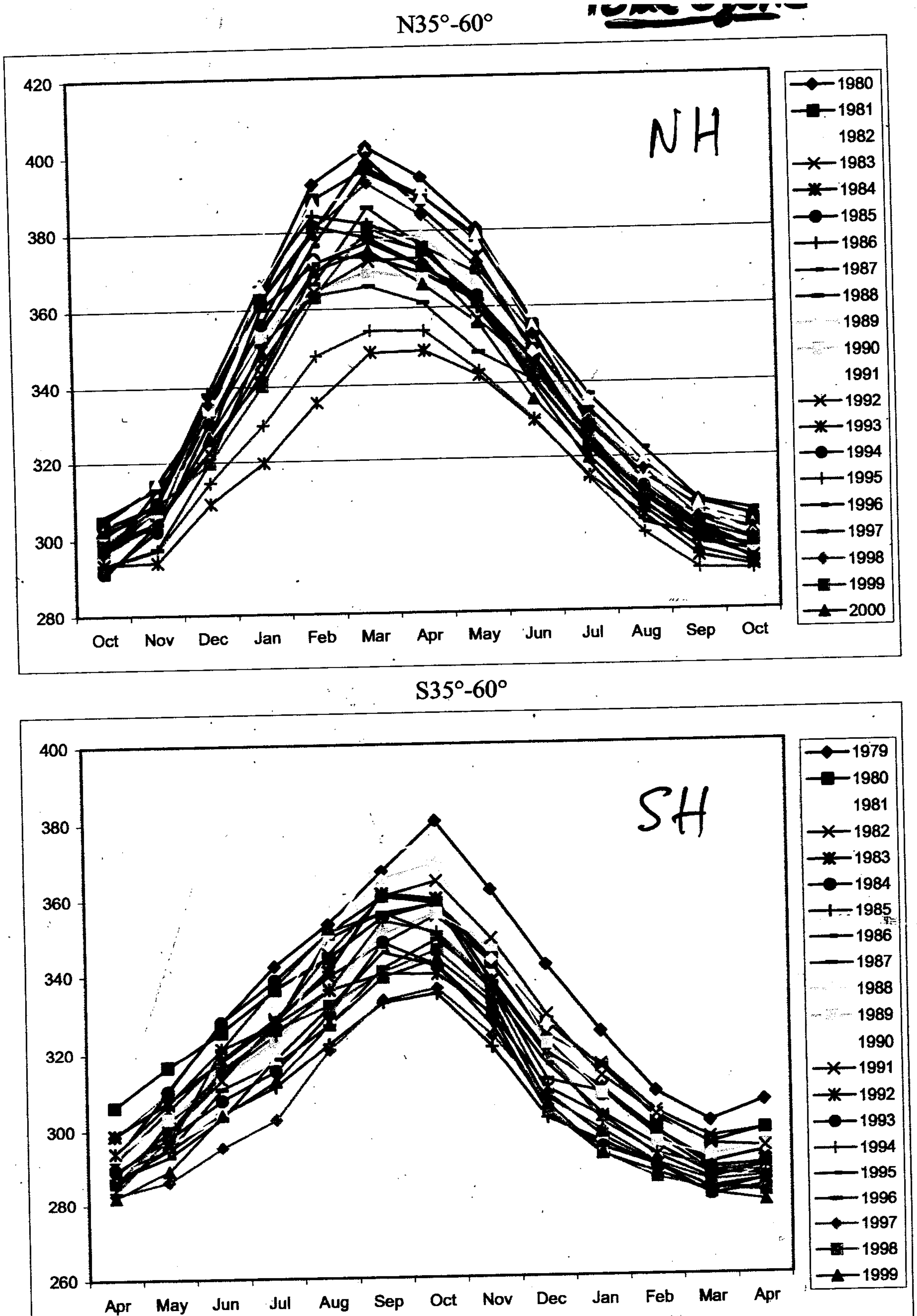

Figure 1. Area weighted total ozone values in DU in different years as a function of the month.

Fioletov & Shepher (GRL 200

http://code916.gsfc.nasa.gov/Data_services/merged

Calculations by Vitali Fioletov (Met. Service of Canada)

Seasonality of regression coefficients with April (NH) and November (SH) → midlatitude total ozone

← NH

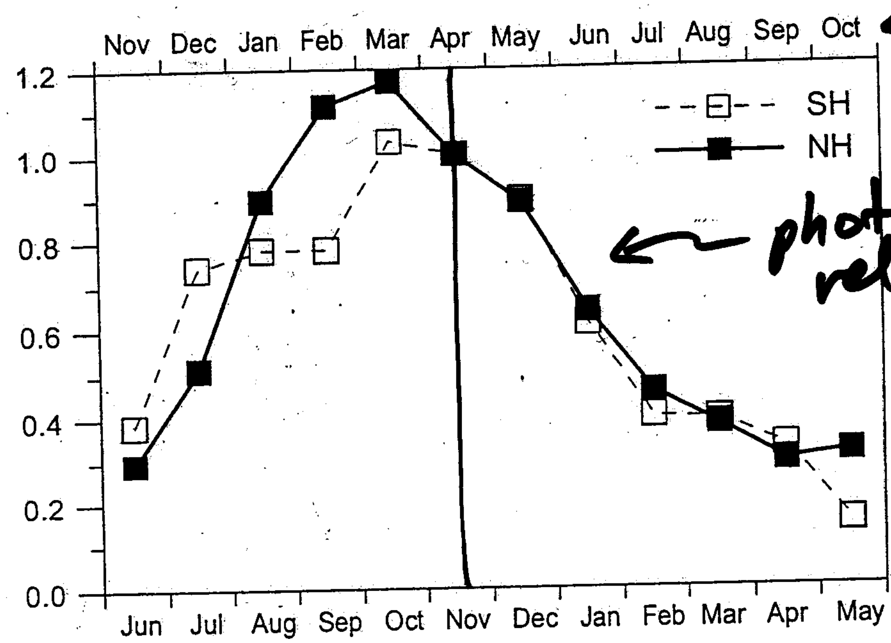

← photochemical relaxation

← SH

Fioletov & Shepherd (GRL 2003)

Figure 5. Linear regression coefficients (solid line with black squares) between ozone departures for April and ozone departures in other month of the year (shown on the top) for the 35°-60°N zone. Similarly, dashed line with open squares shows regression coefficients between November departures and ozone anomalies in other months for the 35°-60°S zone. Detrended data were used.

Calculations by Vitali Fioletov (Met. Service of Canada)

Dynamically-induced interannual variability of extratropical O_3

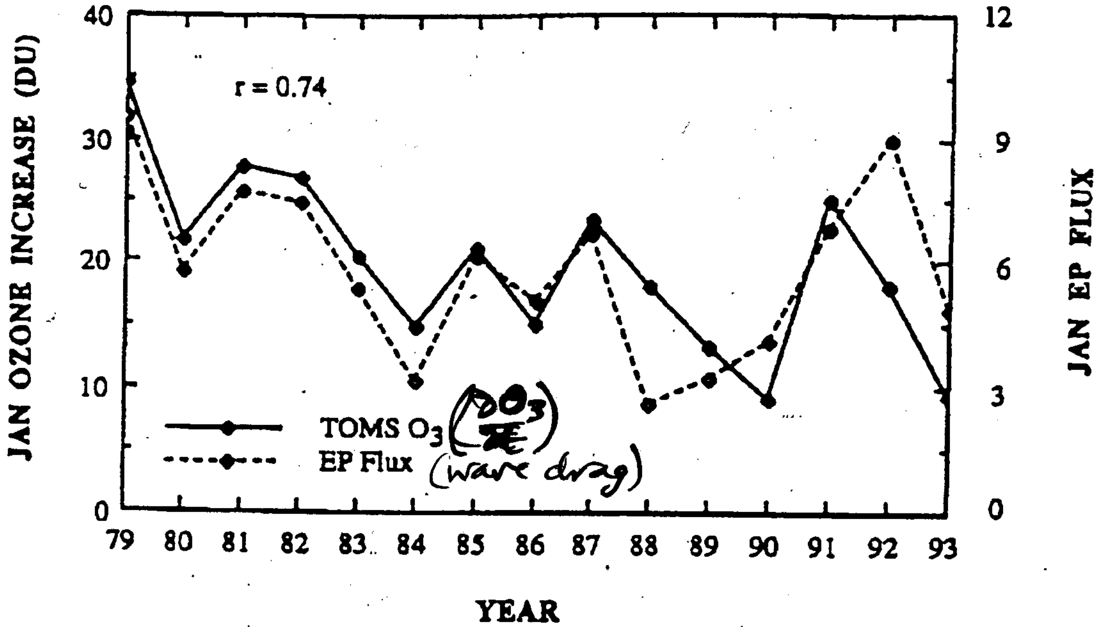

FEBRUARY OZONE

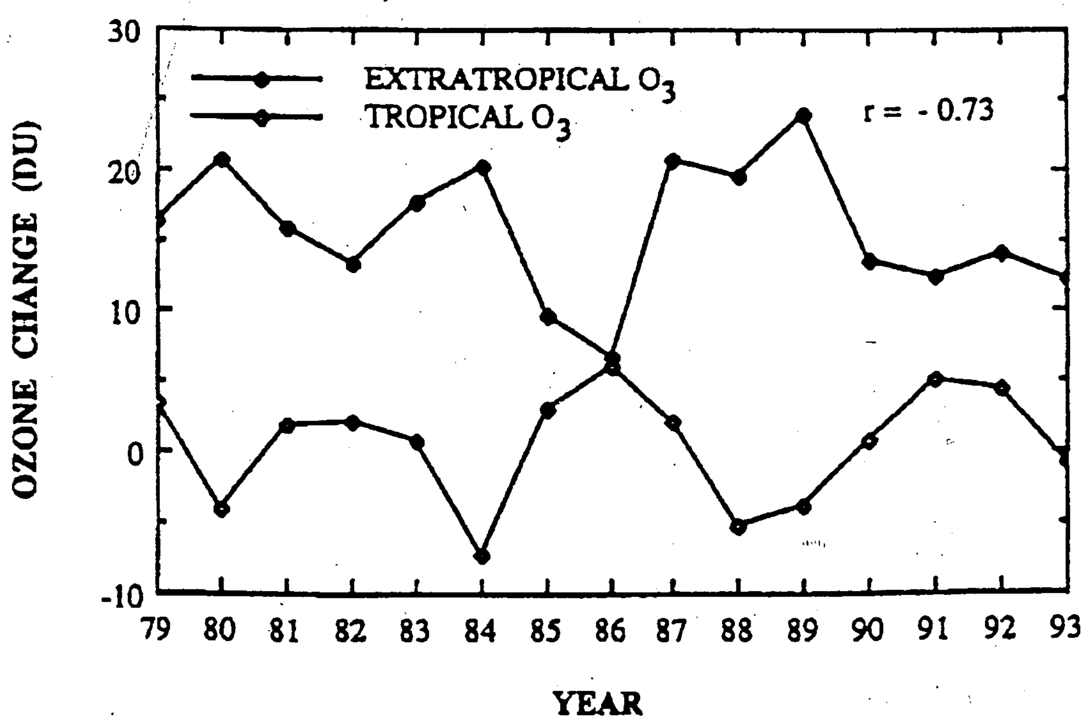

Fusco & Salby (J. Climate 1999)

Randel et al. (JMSJ 2002)

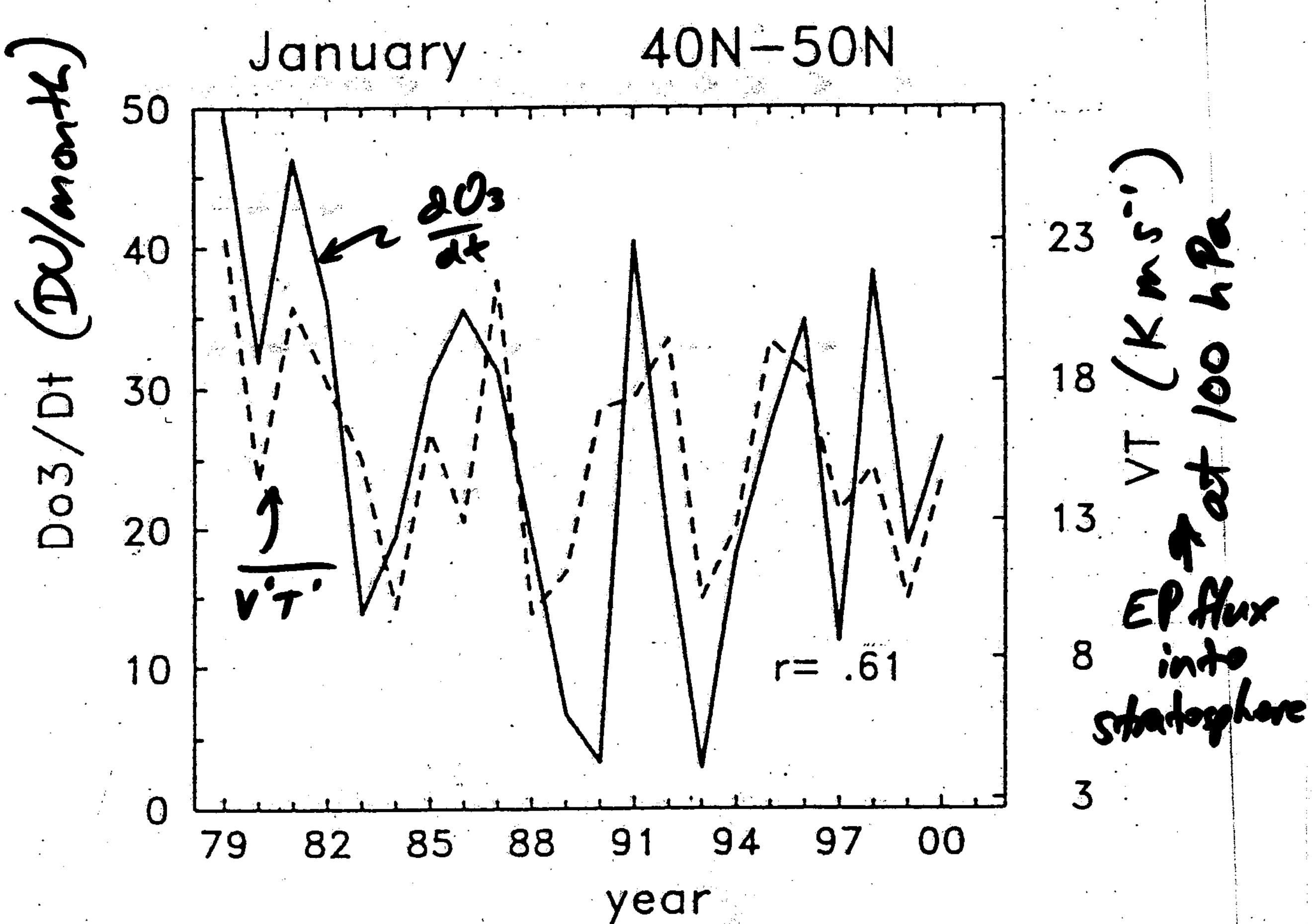

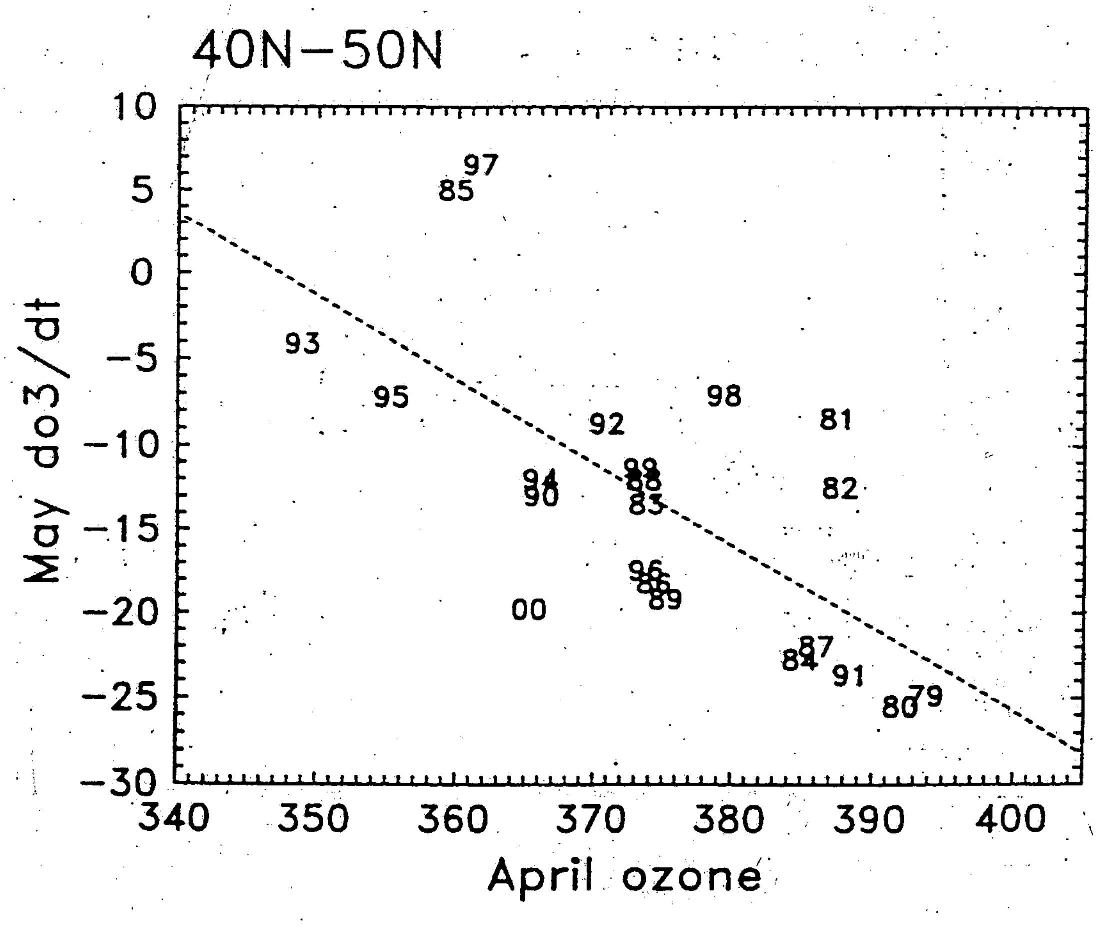

Autocorrelations of total ozone anomalies

(detrended data)

N35°-60°

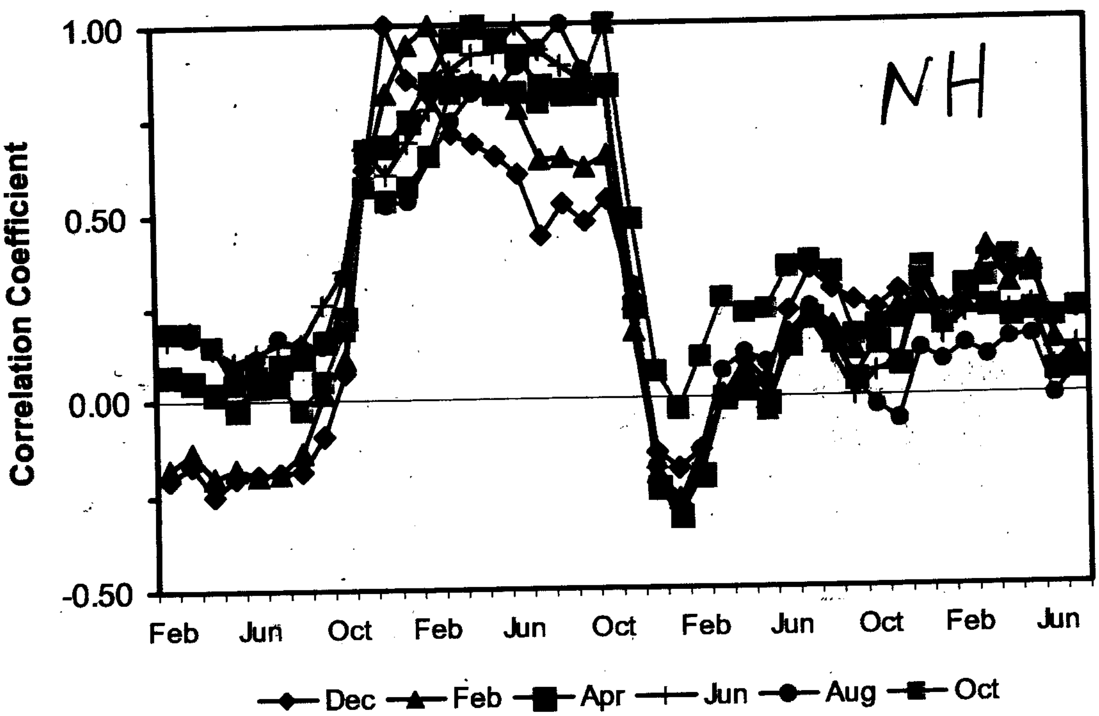

Fioletov & Shepherd (GRL 2003)

S35°-60°

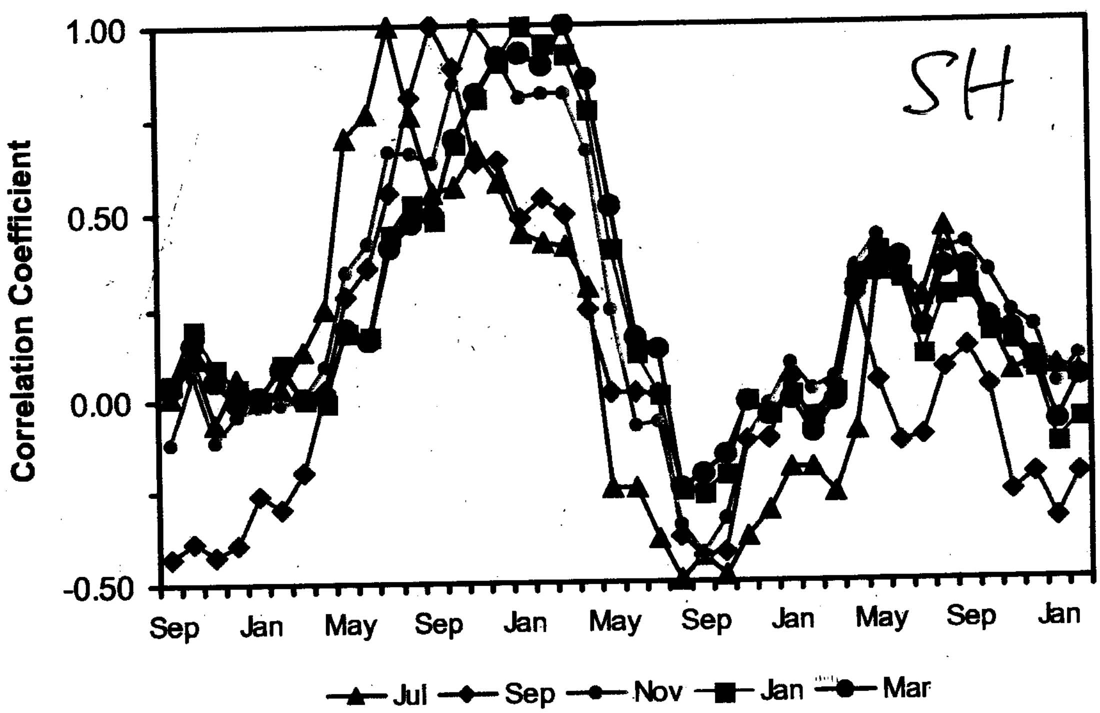

Figure 3. The same as Figure 2, but with monthly data detrended. A linear trend was estimated separately for each month of the year and then subtracted from the data.

Calculations by Vitali Fioletov (Met. Service of Canada)

Ozone deviations from 1979

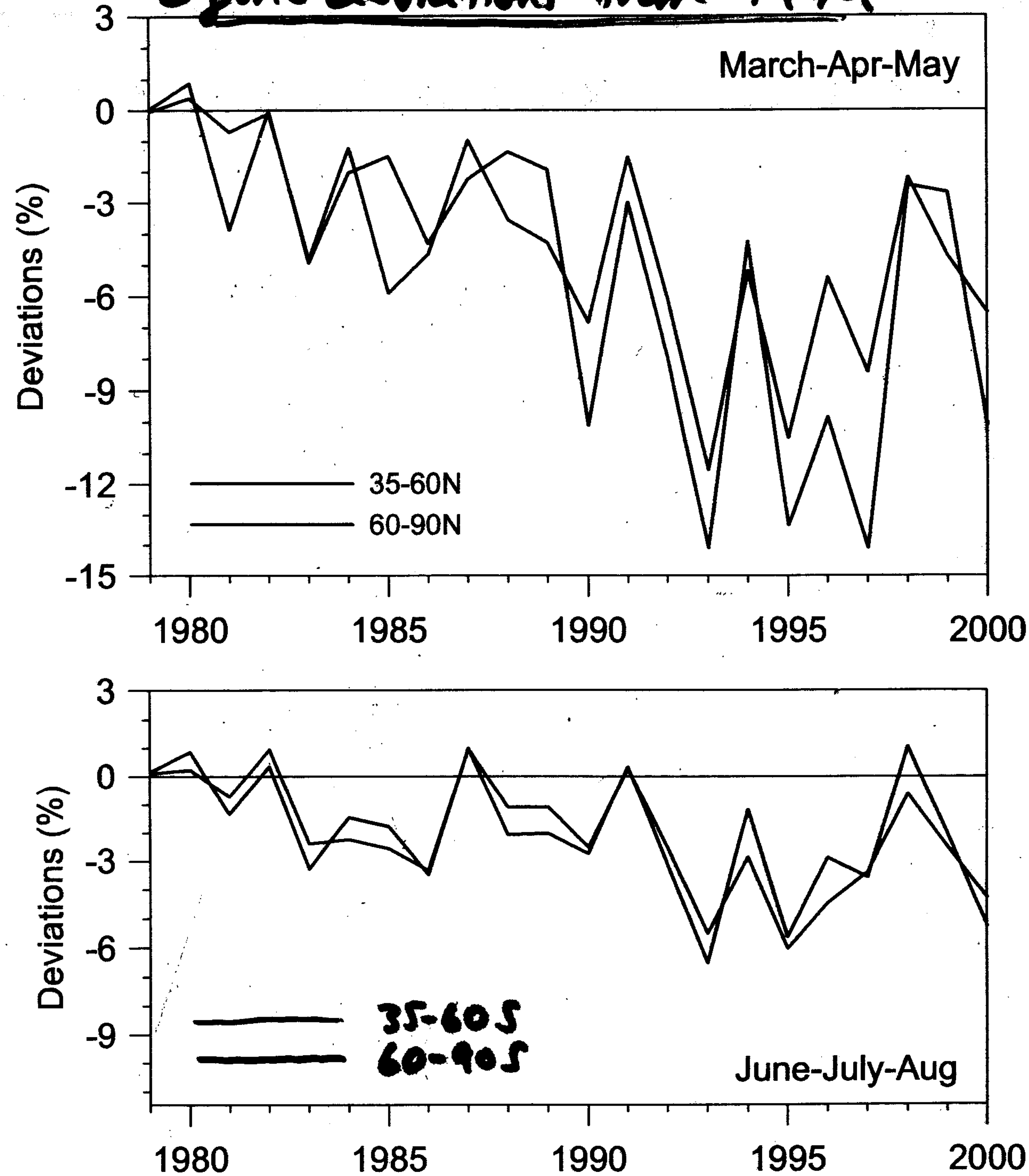

Figure 5. Total ozone deviations for 35-60°N and 60-90°N zones for March-May and June-August. Total ozone variations over the Arctic in general are similar to those over midlatitudes. However, a strong polar vortex in the late winter – early spring yields additional decline in total ozone values. Correlation coefficients between the data plotted at the top and bottom panels are 0.87 and 0.91 respectively.

Calculation by Vitali Fioletov (Met. Service of Canada)

Model O3 Column 47.5 N 92-97 run

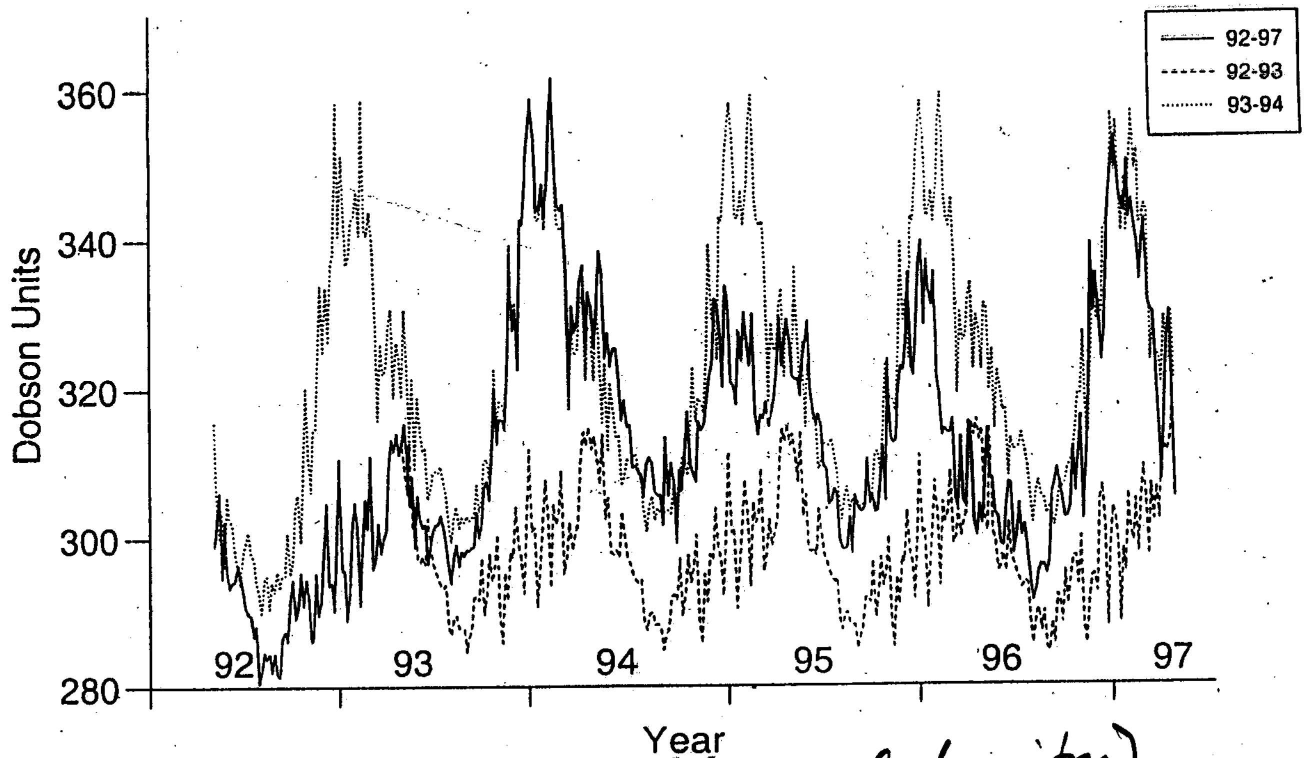

(linearized chemistry)

Chemical transport model run with

- Same meteorology repeated 5 times (2 different years)
- Actual meteorology from 1992-97

→ Variability in ozone controlled by meteorology

Hadjinicolaou et al. (GRL 1997)

Ozone-temperature correlations in a planetary wave as seen by CRISTA 2 (August 15, SH)

Courtesy of William Ward and the CRISTA team (Ward et al., 2000)
(red is high, blue is low)

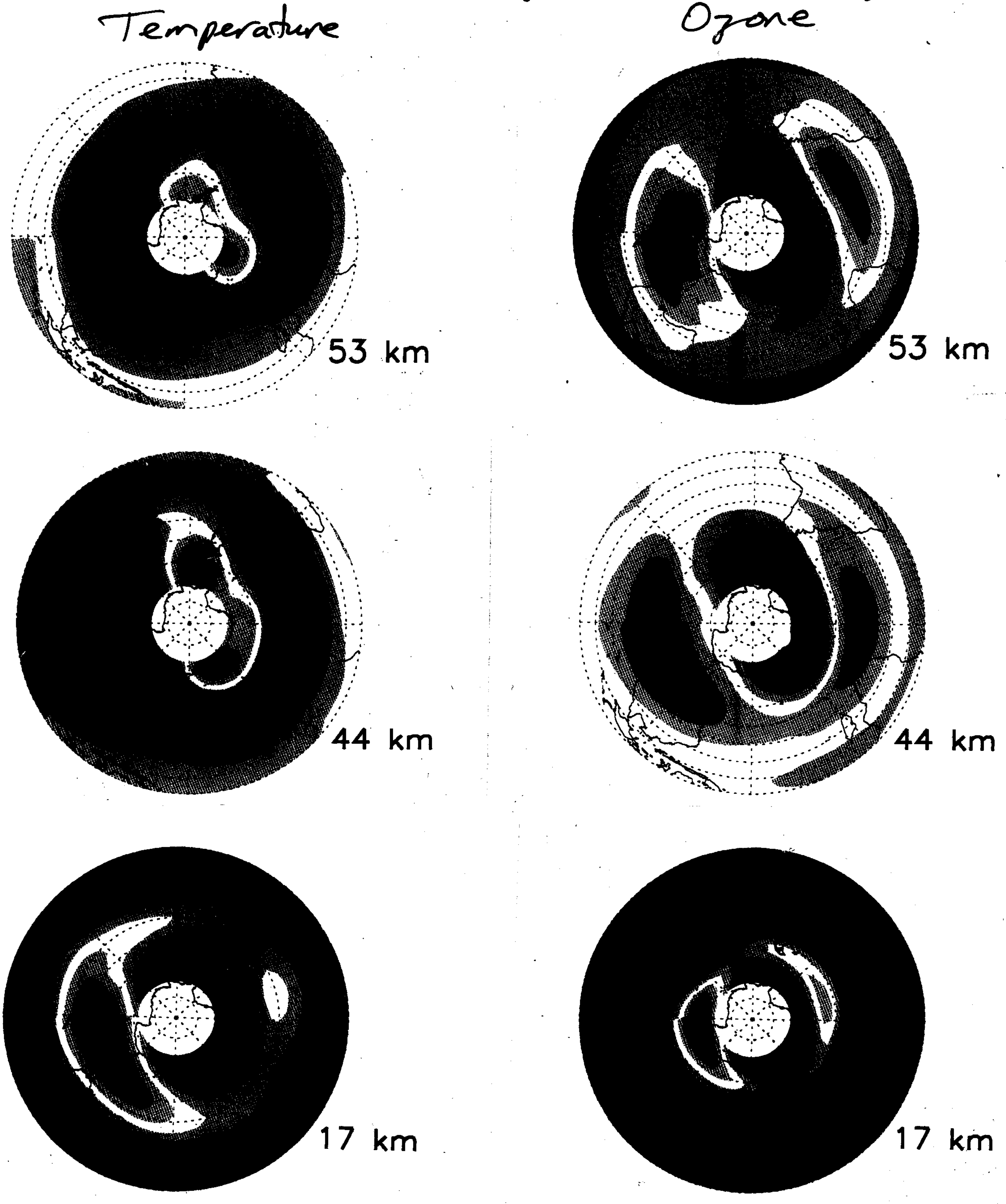

Ozone decline over Halley Bay, Antarctica

Farman et al. (1985)

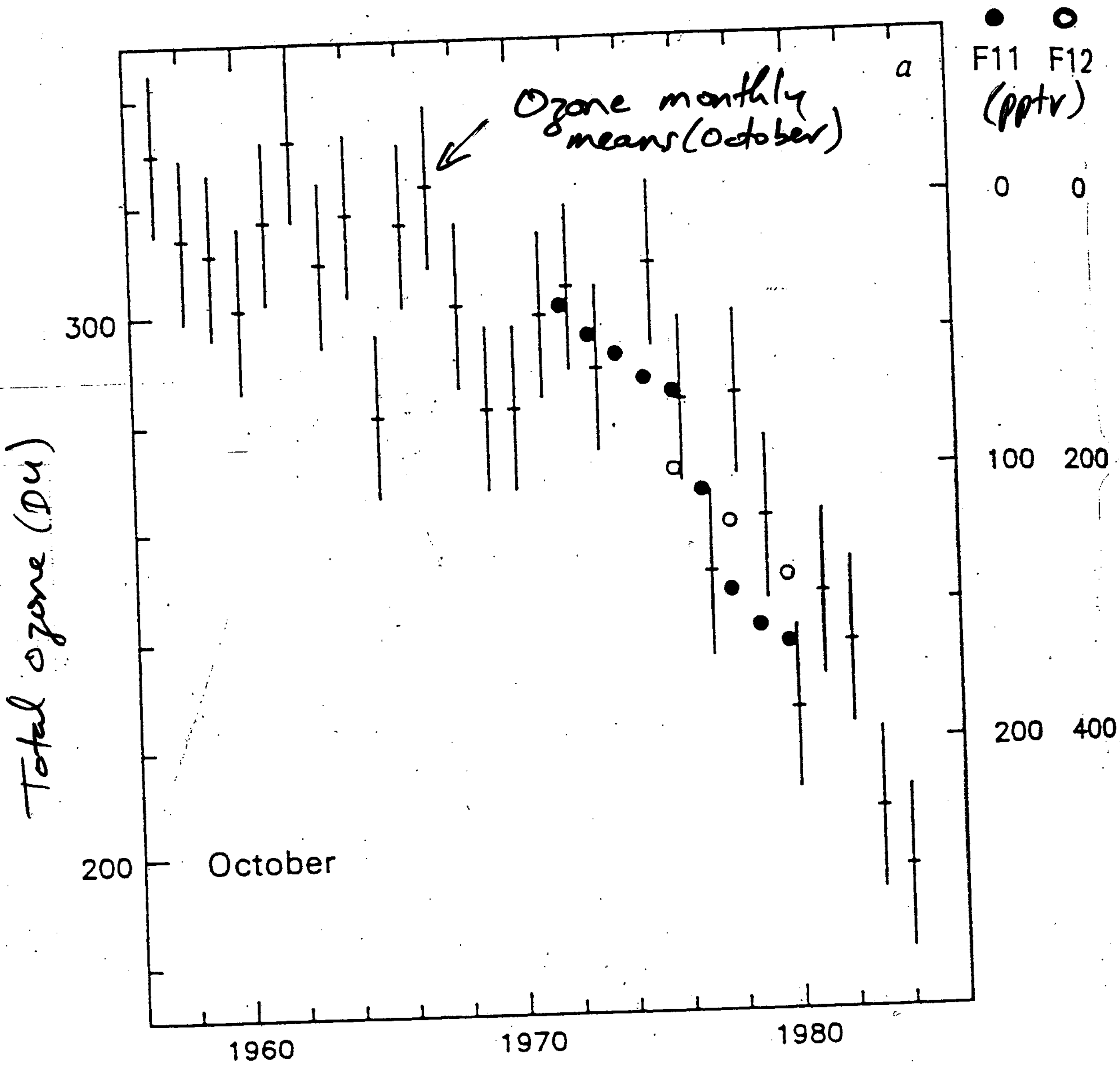

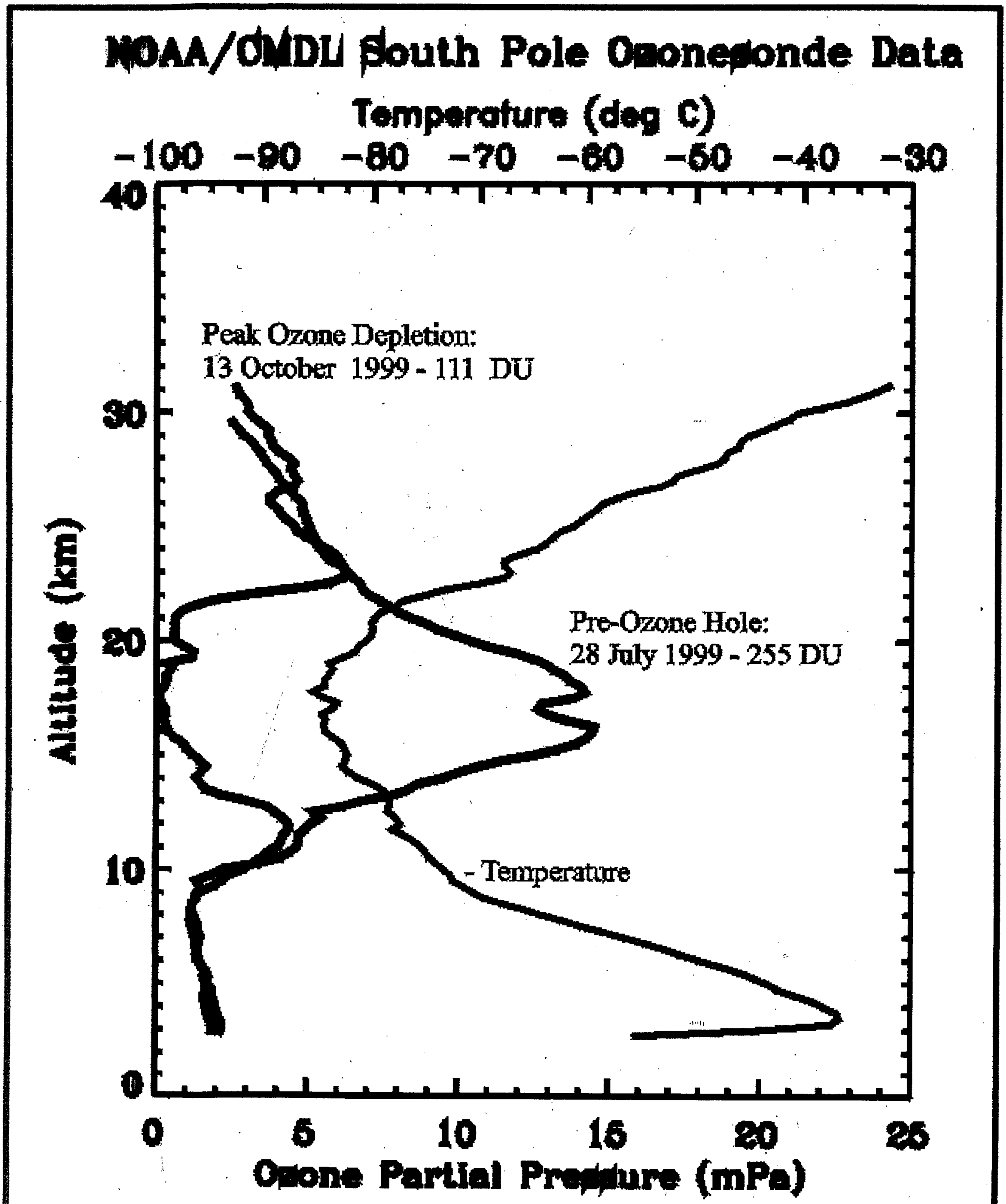
NOAA/CMDL South Pole Ozonesonde Data
Temperature (deg C)
-100 -90 -80 -70 -60 -50 -40 -30
40
30
20
10
0
Altitude (km)
Peak Ozone Depletion:
13 October 1999 - 111 DU
Pre-Ozone Hole:
28 July 1999 - 255 DU
- Temperature
0 5 10 15 20 25
Ozone Partial Pressure (mPa)

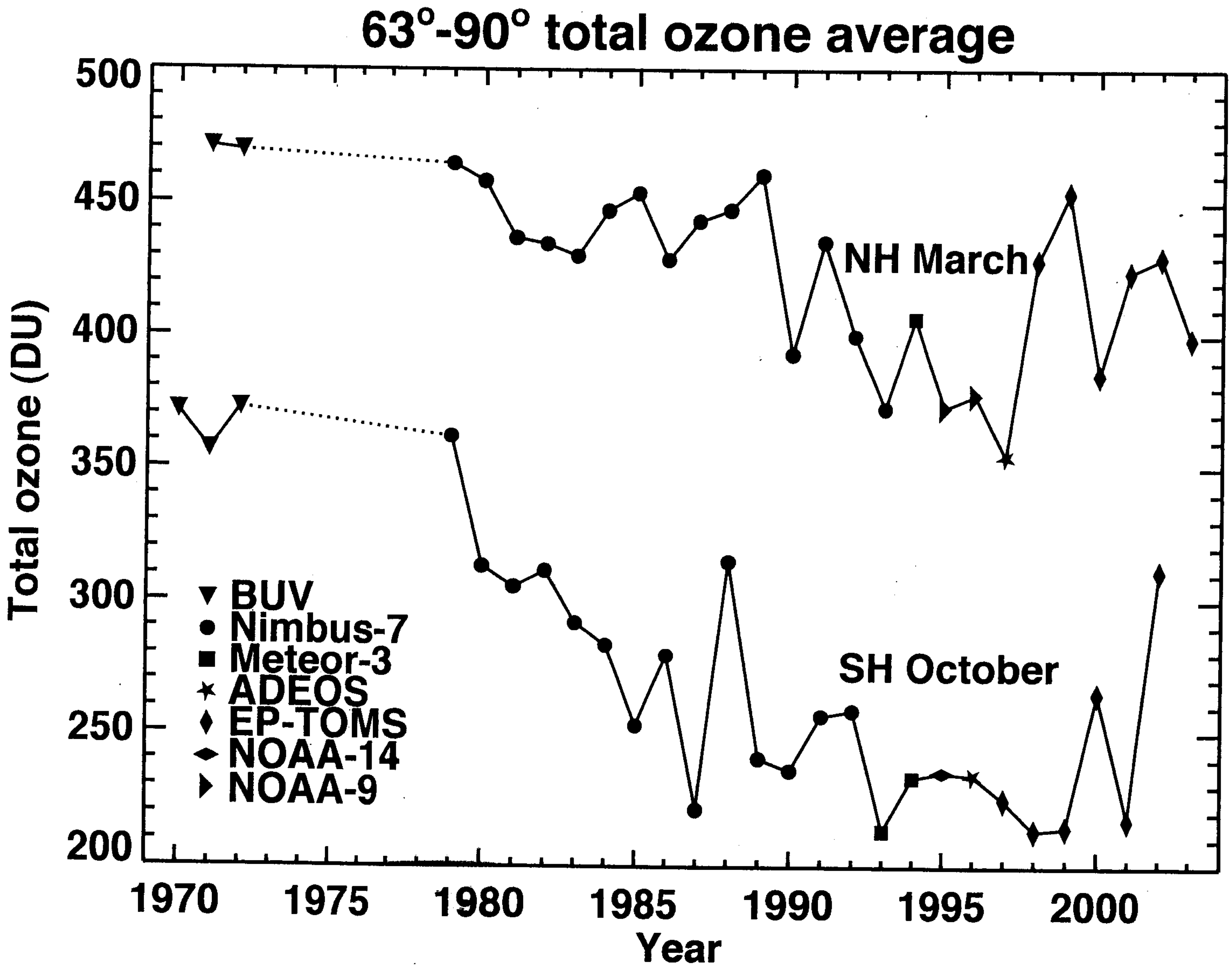

Courtesy of Paul Newman (NASA GSFC)

Low temperatures and low ozone: which causes which?

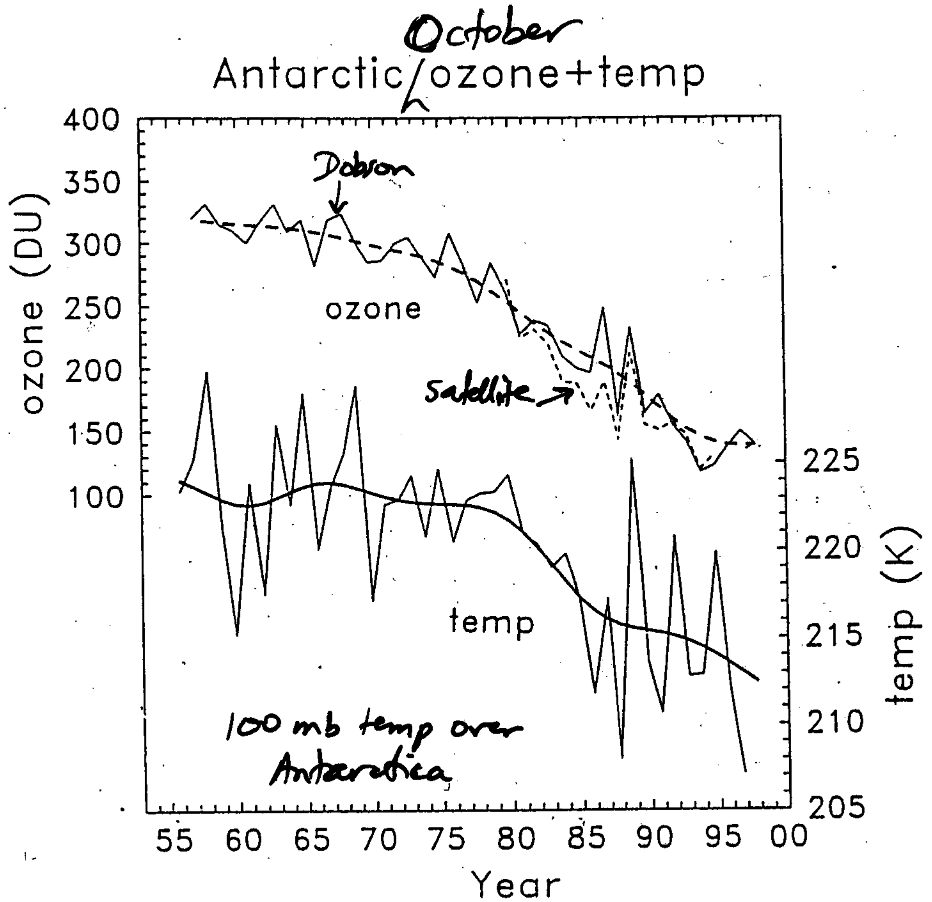

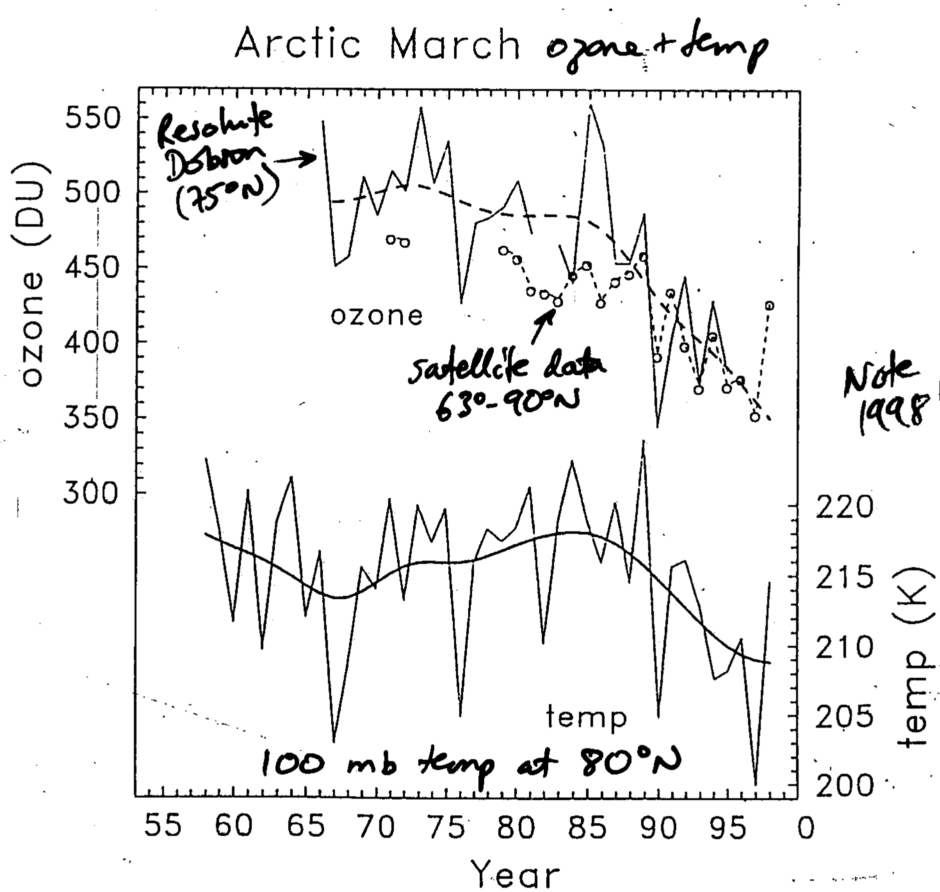

Note 1998!

from Randel & Wu (1999, J. Clim.)

March total ozone

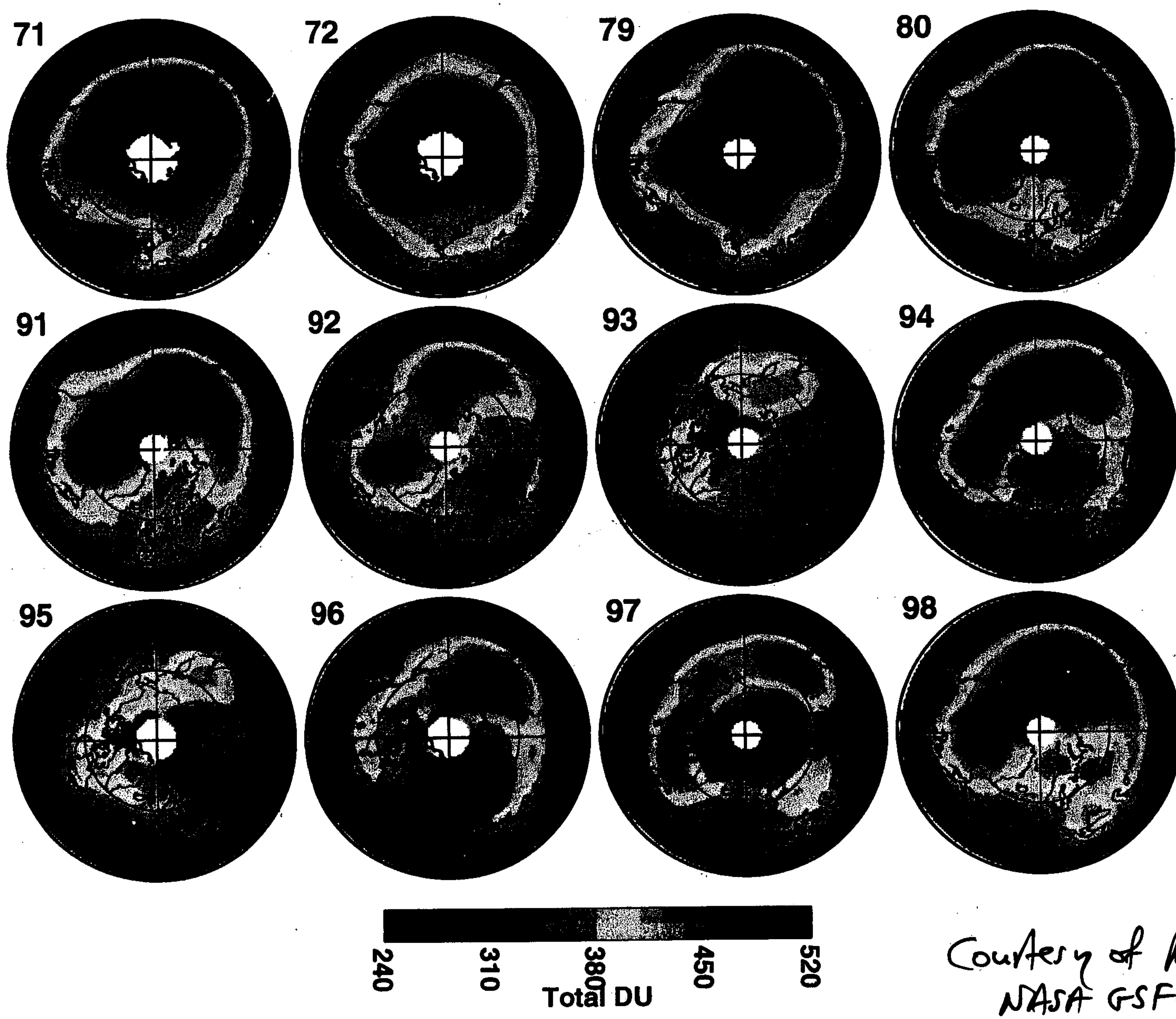

Courtesy of Paul Newman
NASA GSFC

17

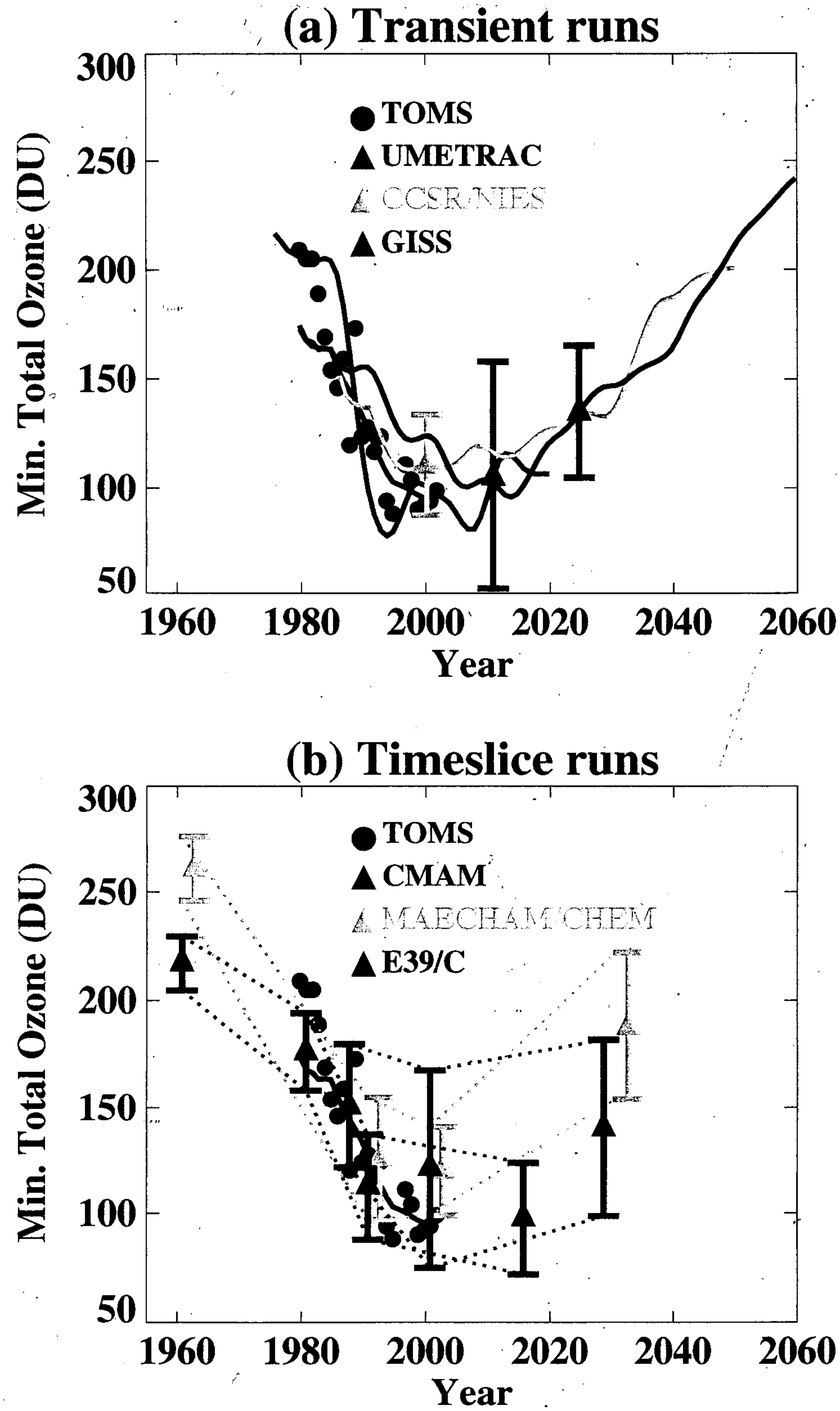

Fig. 10. As in Fig. 9, but for the minimum Antarctic ozone, September to November. For MAECHAM/CHEM only: (i) the values have been plotted two years late for clarity, (ii) a standard tropospheric column of 40 DU has been added to the computed columns above 90 hPa.

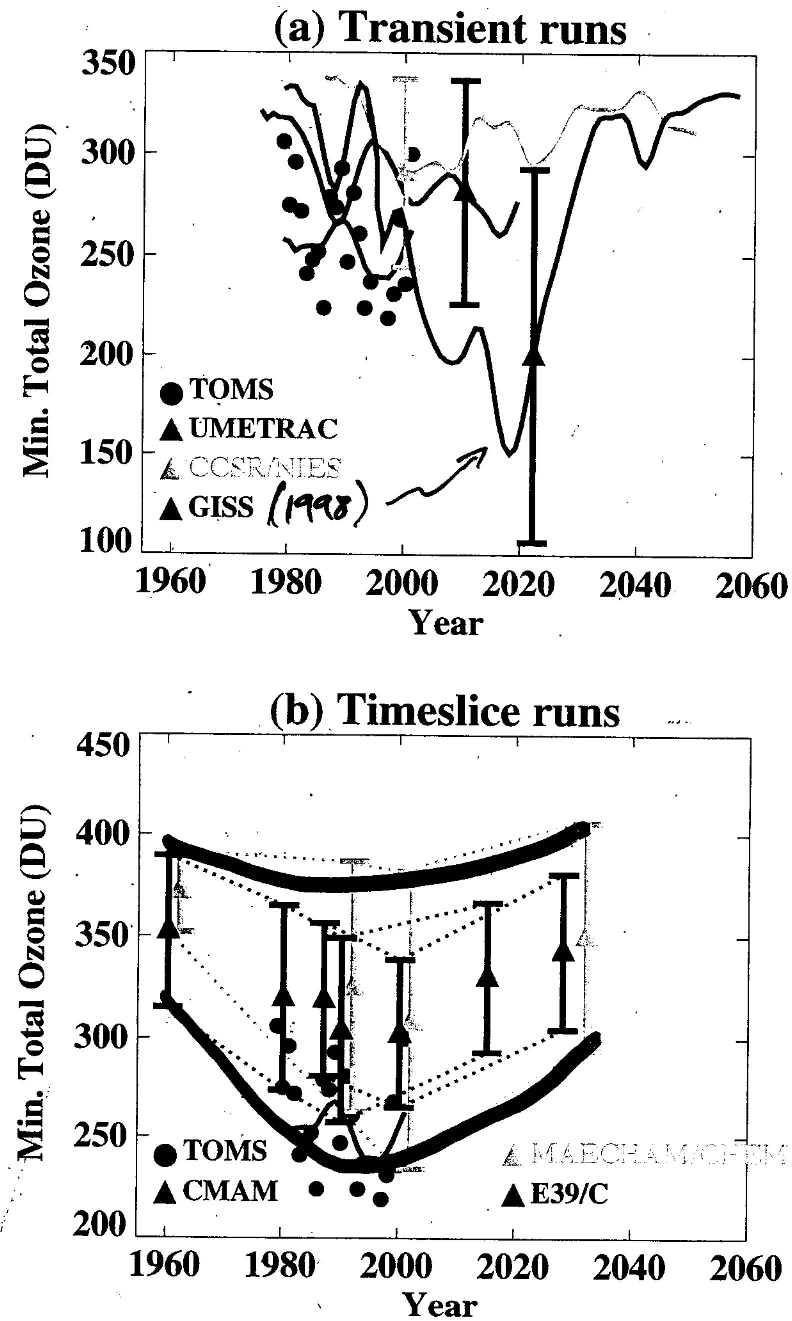

Fig. 9. Minimum Arctic (March/April) total ozone for the main experiments of this assessment. **(a)** Transient runs in comparison with TOMS data. The solid lines show the results of a guassian smoother applied to the individual year's results. The error bars denote twice the standard deviation of the individual years from the smoothed curve. **(b)** Time slice runs in comparison with TOMS data. The error bars denote the mean and twice the standard deviation of the individual years within each model sample (10 years for CMAM, 20 years for MAECHAM/CHEM and E39/C). Dotted lines are drawn between the end points of the error bars to assist in estimating trends by eye. For MAECHAM/CHEM only: (i) the values have been plotted two years late for clarity, (ii) a standard tropospheric column of 100 DU has been added to the computed columns above 90 hPa. Note that the MAECHAM/CHEM results are not symmetric about the mean, but have a long tail towards low values.

Minimum Arctic total O_3 in March/April

Austin et al. (ACP 2003)

Various 2D chemistry models vs. obs

(25-month running mean applied to time series)

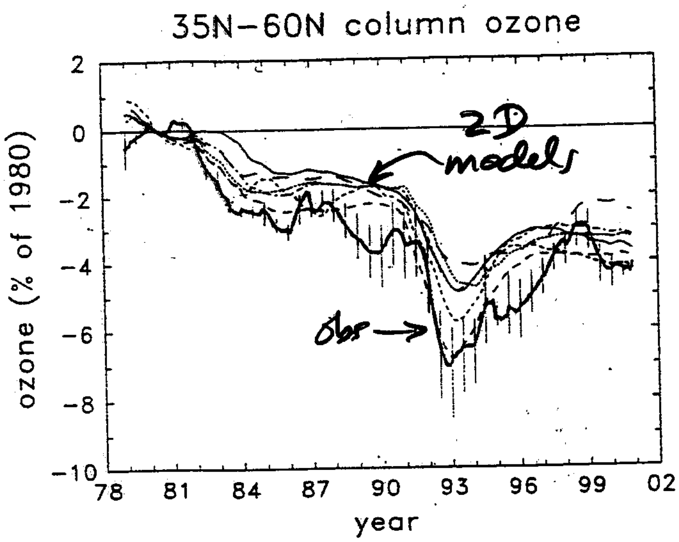

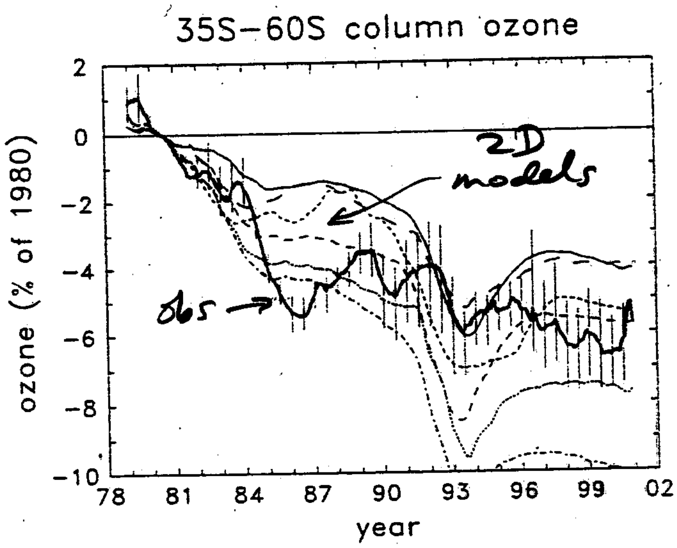

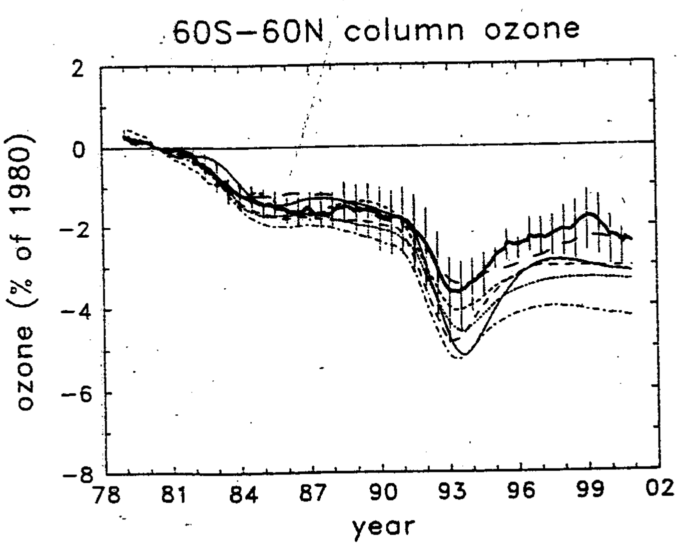

WMO (2003)

Annual cycle of zonal-mean temperature change at 100 hPa between 1979-2000

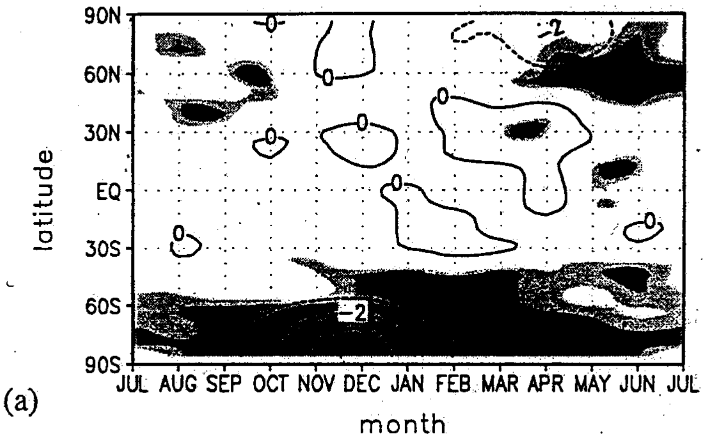

From Berlin model (ΔO_3 only)

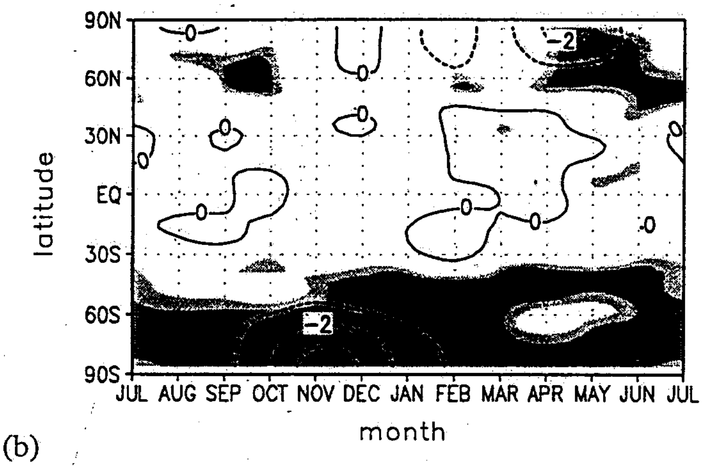

From Berlin model (ΔO_3 and ΔCO_2)

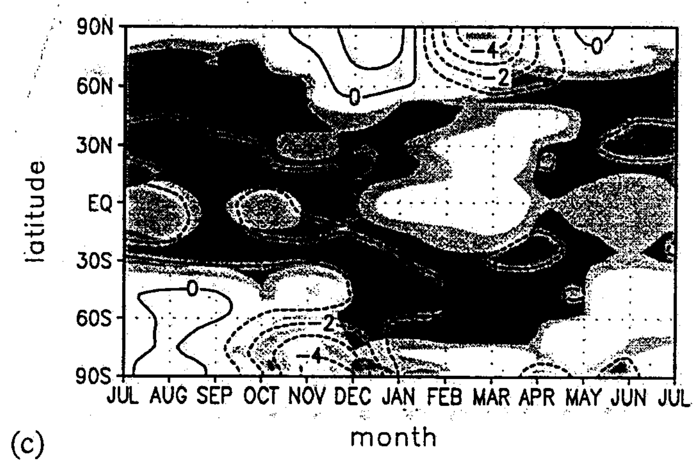

Observed

Figure 3. Annual cycle of the zonal mean temperature change at 100 hPa a) simulated by the FUB CMAM for the observed ozone decrease, b) like a) but with additional CO_2 increase and c) derived from the NCEP/NCAR-Reanalyses of the period 1979-2000 (contour interval 1 K/decade). Dark (light) shaded areas denote regions where the trends are significant at the 99% (95%) level.

Langematz et al. (JGR 2002)

Annual and zonal-mean temperature trends from 1979-1997 at 50 hPa

(various models forced by observed ozone trends)

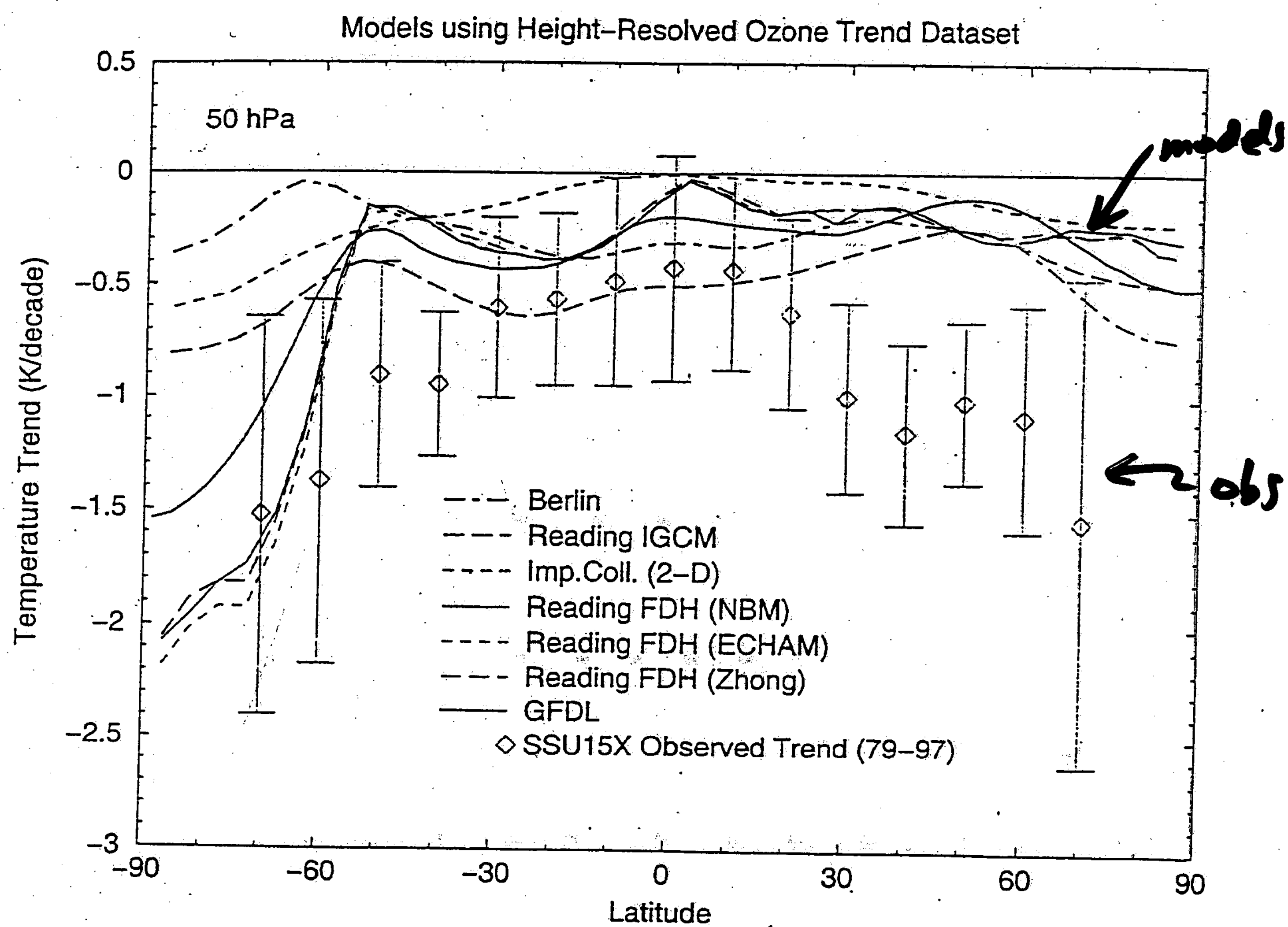

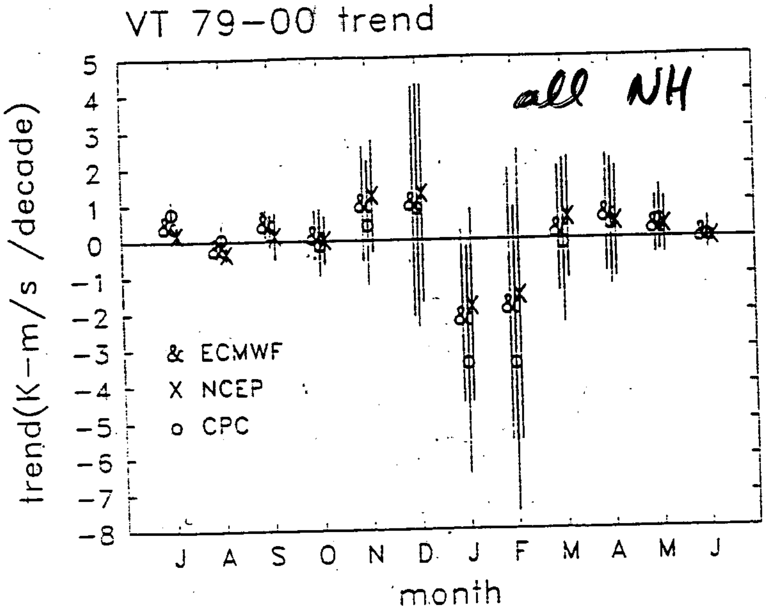

NH integral of $\overline{v'T'}$ at 100 hPa (EP flux into stratosphere) = stratospheric wave forcing (PWD)

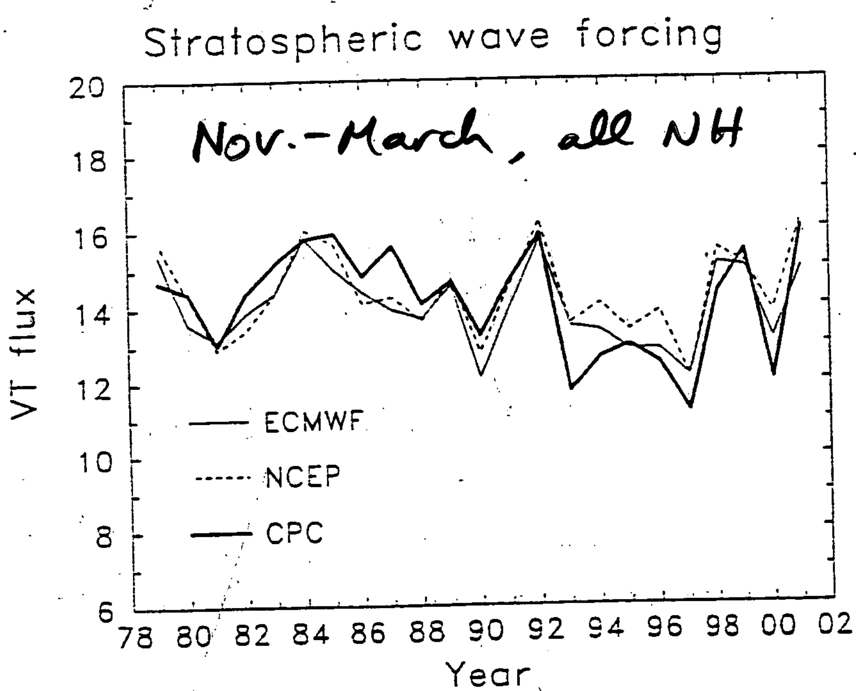

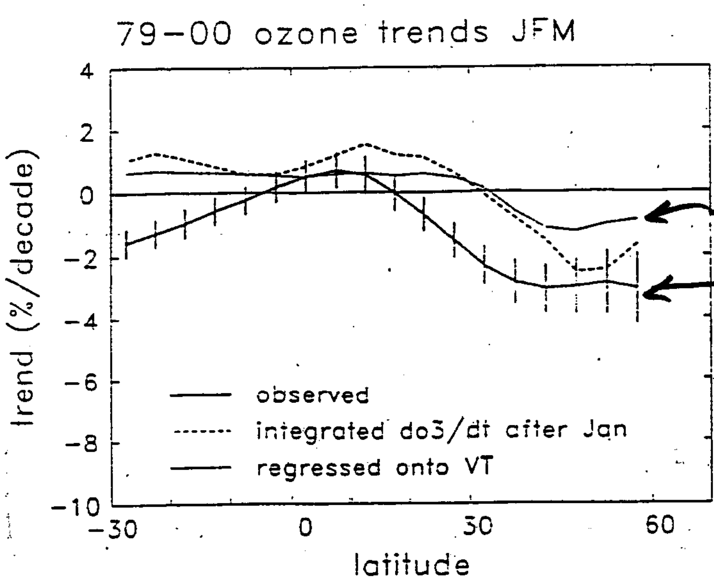

← statistically assoc'd with PWD trend

← observed

Randel et al. (2002 JMSJ)

2D model simulations of (non-polar) ozone recovery

COLUMN O_3

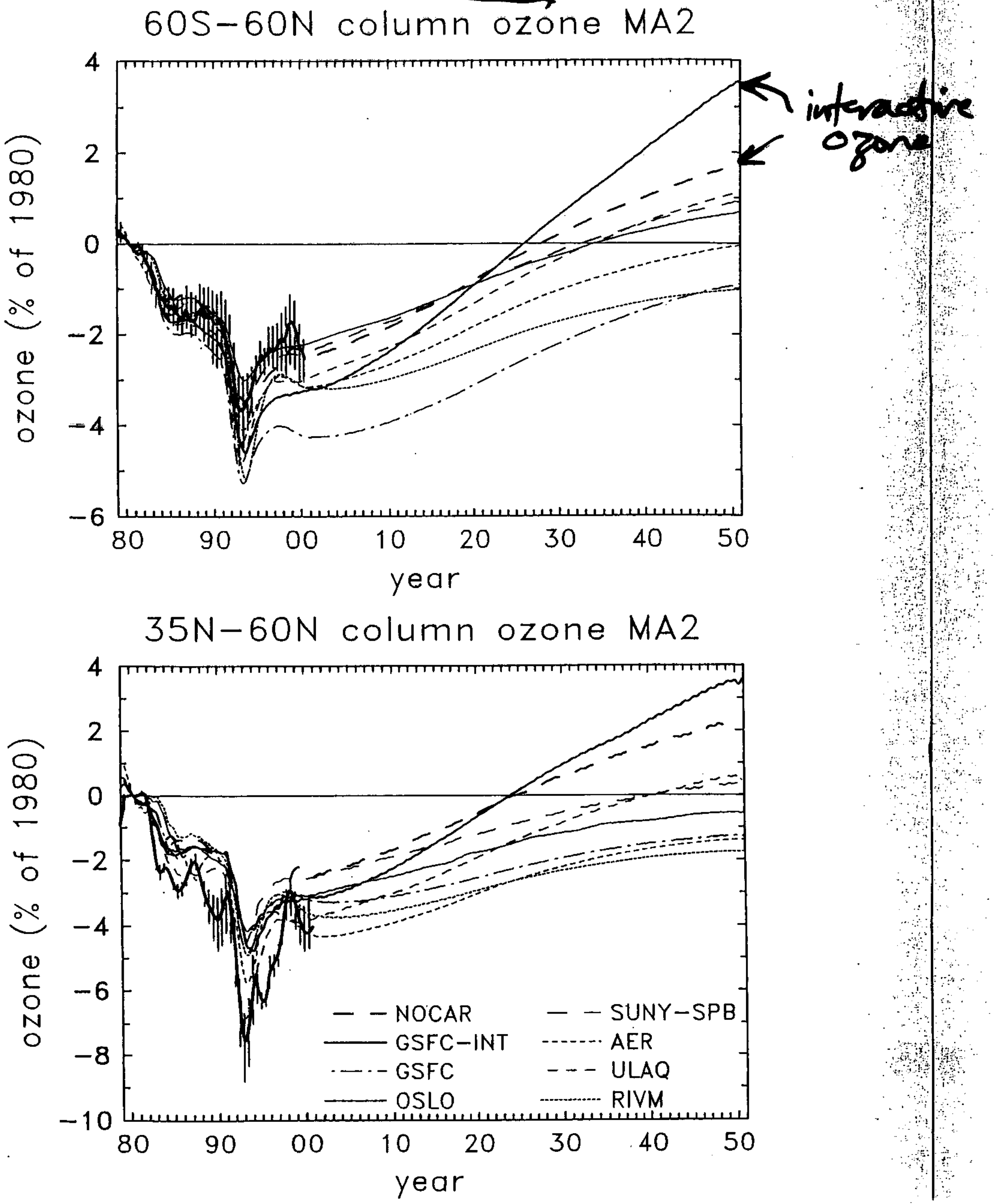

UPPER STRAT O_3

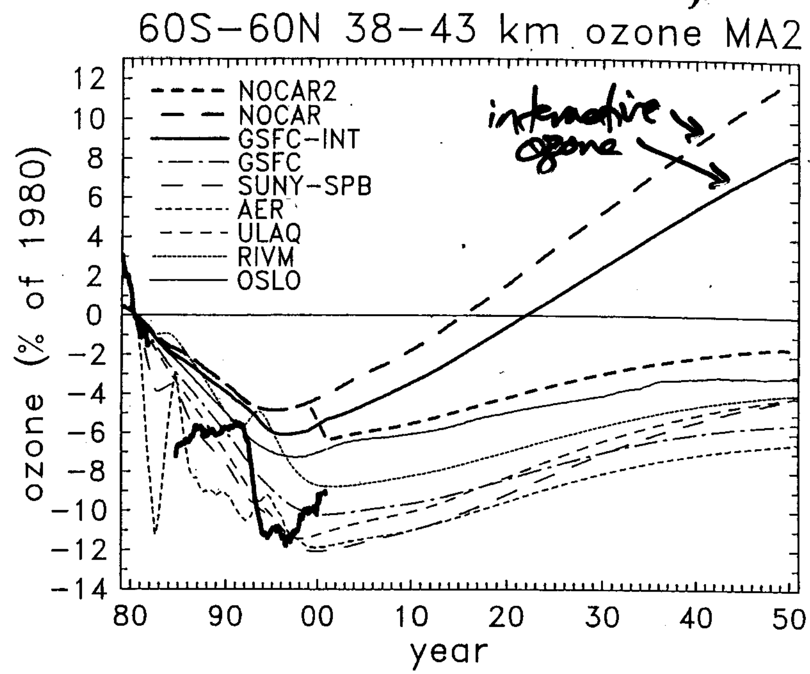

Figure 4-43. Predicted future evolution of US ozone (38-43 km), averaged over latitudes 60°S-60°N from the eight 2-D models shown in Figure 4-42. An additional model run (labeled NOCAR2) used the NOCAR model but with fixed CO_2 after 2000 (with CO_2 set to 1980 values, accounting for the discontinuity near 2000). The models used GHG scenario MA2. The plots also include the model results and observations (SAGE I+II; red lines) of past changes prior to 2000 (see Section 4.5.3).

WMO (2003)

Time evolution of stratospheric wave driving

Models forced by changing halogens and GHGs

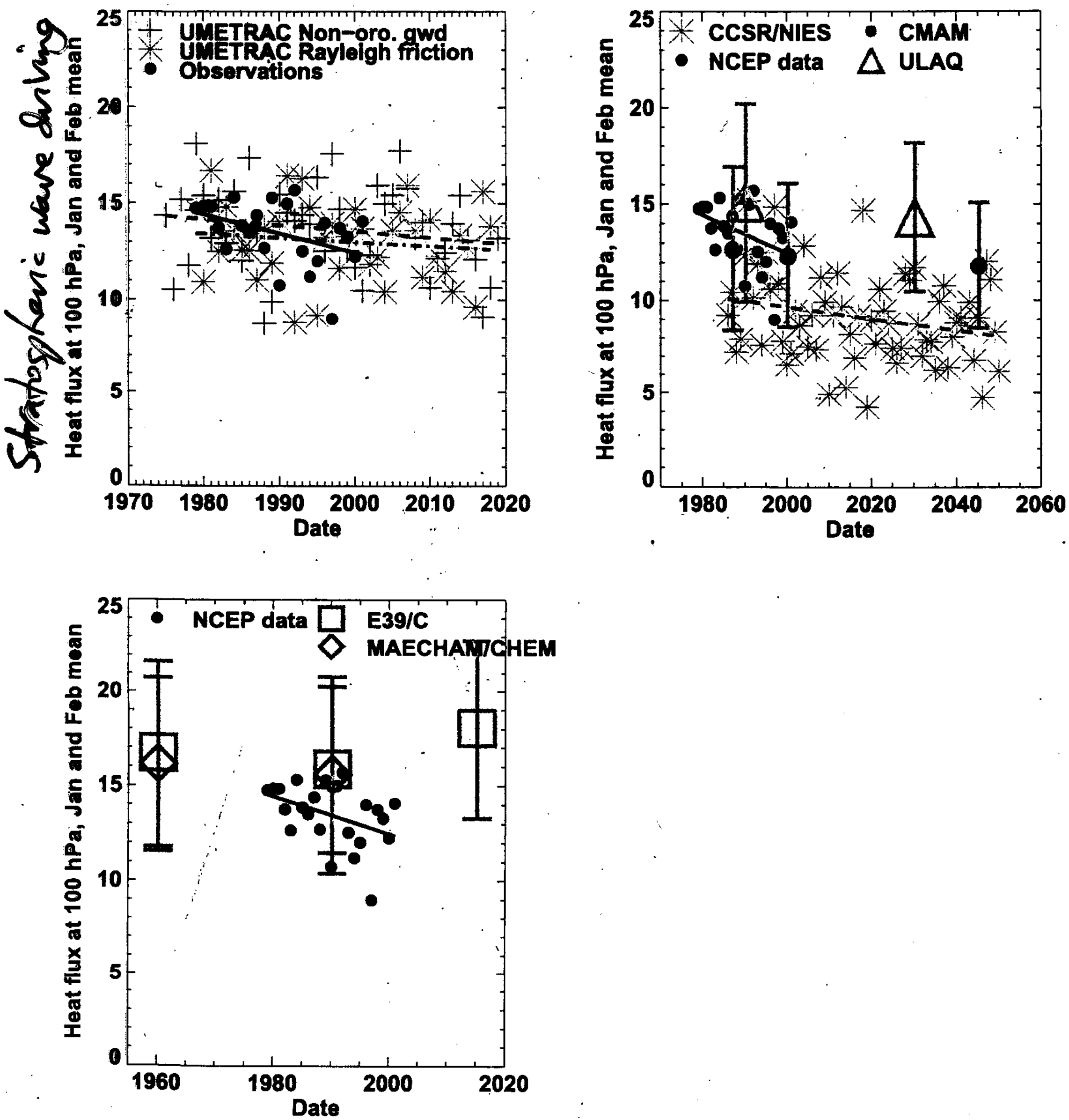

Fig. 8. Scatter diagrams of heat flux $\overline{v'T'}$ (averaged 40°–80° N, at 100 hPa for January and February) against year for participating models. In all panels, the linear regression line between the NCEP derived heat flux and time is drawn as a solid line. Upper left panel: the dashed line is the linear regression for the non-orographic gwd run of UMETRAC, and the dot-dash line is the linear regression for the Rayleigh friction run of UMETRAC. Upper right panel: the dashed line is the linear regression for the CCSR/NIES results. Two standard deviations of the annual values are indicated by the error bars for the time slice experiments. For CMAM, the results are plotted for 2045 rather than 2028 since the results are dependent largely on the WMGHG concentrations (see Sect. 2.1).

Austin et al. (ACP 2003)

30 hPa North Pole temperature over the last 50 years (Berlin analysis)

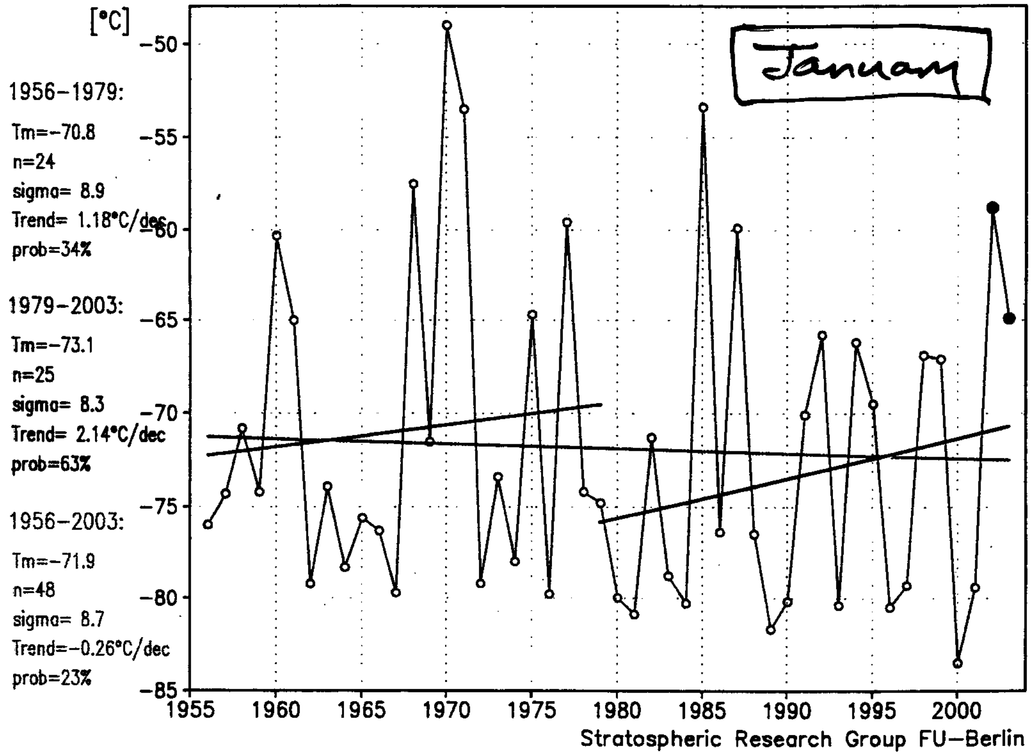

Figure 5. Time series of the monthly mean 30-hPa North Pole temperatures (° C) in January, 1956–2003. Different trends are indicated. Data: Free University Berlin, ECMWF: 2002 + 2003. ([15], updated).

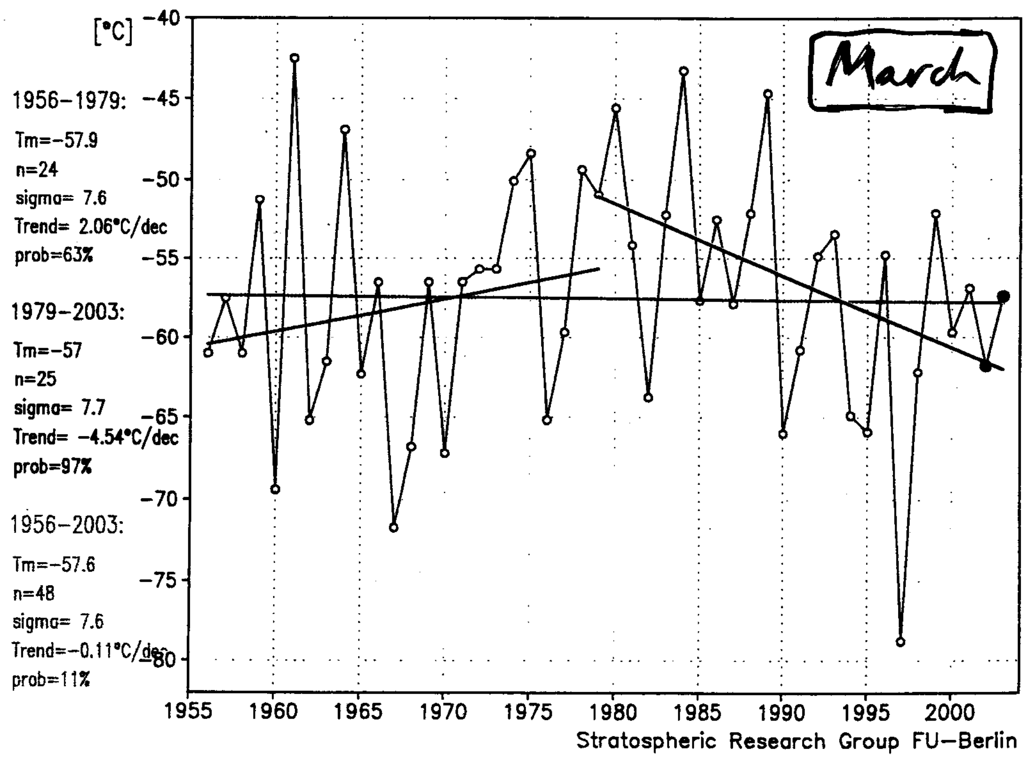

Figure 6. as Fig. 5, but for March.

FU-Berlin